Please cite as: Maccallini, C.; Di Matteo, M.; Gallorini, M. et al. (2018), “Discovery of N-{3-[(ethanimidoylamino)methyl]benzyl} -l-prolinamide dihydrochloride: A new potent and selective inhibitor of the inducible nitric oxide synthase as a promising agent for the therapy of malignant glioma”, European Journal of Medicinal Chemistry, Volume 15, pp. 53-64, doi:10.1016/j.ejmech.2018.04.027.

Discovery of *N*-{3-[(ethanimidoylamino)methyl]benzyl}-L-prolinamide dihydrochloride: a New Potent and Selective Inhibitor of the Inducible Nitric Oxide Synthase as a Promising Agent for the Therapy of Malignant Glioma

Cristina Maccallini, †* Mauro Di Matteo, † Marialucia Gallorini, † Monica Montagnani, ‡ Valentina Graziani, † Alessandra Ammazzalorso, † Pasquale Amoia, † Barbara De Filippis, † Sara Di Silvestre, § Marialuigia Fantacuzzi, † Letizia Giampietro, † Maria A. Potenza, ‡ Nazzareno Re, † Assunta Pandolfi, § Amelia Cataldi, †Rosa Amoroso.†

†Department of Pharmacy - University of Chieti "G. d'Annunzio", Italy
‡ Department of Biomedical Sciences and Human Oncology, Medical School - University of Bari "Aldo Moro", Italy
§ Department of Medical, Oral and Biotechnological Sciences, Centro Scienze dell'Invecchiamento e Medicina Traslazionale (Ce.SI-MeT), University "G. d'Annunzio" Chieti-Pescara, Italy.

Corresponding Author

* Cristina Maccallini, cristina.maccallini@unich.it

HIGHLIGHTS

- iNOS appears a key regulator of malignant astrocytes transformations and of tumor cells proliferation and iNOS inhibition might have potential therapeutic value in the treatment of gliomas.
- A new series of acetamidines was synthesized, and molecule **39** gave potent and selective iNOS inhibition.
- The selectivity of action of **39** was *ex-vivo* confirmed
- Molecule **39** was cytotoxic and antiproliferative against C6 rat glioma cells .

GRAPHICAL ABSTRACT

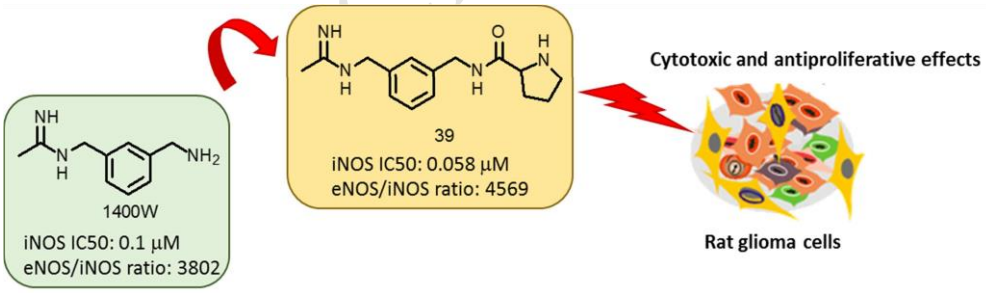

Abstract

In mammalian cells, aberrant iNOS induction may have detrimental consequences, and seems to be involved in the proliferation and progression of different tumors, such as malignant gliomas. Therefore, selective inhibition of iNOS could represent a feasible therapeutic strategy to treat these conditions. In this context, we have previously disclosed new acetamidines able to inhibit iNOS with a very high selectivity profile over eNOS or nNOS. Here we report the synthesis of a new series of compounds structurally related to the leading scaffold of N-[(3-aminomethyl)benzyl] acetamidine (1400W), together with their *in vitro* activity and selectivity. Compound **39** emerged as the most promising molecule of this series, and it was *ex vivo* evaluated on isolated and perfused resistance arteries, confirming a high selectivity toward iNOS inhibition. Moreover, C6 rat glioma cell lines biological response to **39** was investigated, and preliminary MTT assay showed a significant decrease in cell metabolic activity of C6 rat glioma cells. Finally, results of a docking study shed light on the binding mode of **39** into NOS catalytic site.

KEYWORDS. Acetamidine; Anticancer; Docking; Glioma; Inhibitors; Nitric Oxide; Nitric Oxide Synthases; Synthesis.

ABBREVIATIONS

NO, Nitric Oxide; eNOS, endothelial Nitric Oxide Synthase; iNOS, inducible Nitric Oxide Synthase; nNOS, neuronal Nitric Oxide Synthase; Boc, ter-butyloxycarbonyl; iBuOCOCl, iso-Butylchloroformate; NMM, N-Methylmorpholine; NA, Noradrenaline; L-NAME, Nω-Nitro-L-arginine methyl ester; MVA, mesenteric vascular arteries; MTT, 3-(4,5-dimethylthiazol-2-yl)-2,5-diphenyltetrazolium bromide; LDH, lactate dehydrogenase.

1. Introduction

Endogenous nitric oxide (NO) is a pleiotropic radical molecule, produced by Nitric Oxide Synthases as a by- product of the conversion of L-Arginine to L-Citrulline [1]. There are three isoforms of NOS: the constitutively expressed neuronal (nNOS or NOS1) and endothelial (eNOS or NOS3) ones, and the non-constitutive, inducible NOS (iNOS or NOS2). When activated, the constitutive NOSs are responsible for the production of low and regulated levels of NO, while iNOS generates higher amounts of NO and for protracted periods. Indeed, basically, iNOS is implicated in the immune response, while the constitutive isoforms play essential roles in several tissues, being involved, for example, in atypical neurotransmission, synaptic plasticity, and in the protection of the cardiovascular system [2]. However, a dysregulated production of NO by a given NOS isoform has been implicated in the development of different diseases, such as neurodegeneration [3], migraine [4], asthma [5], chronic bowel disease [6], cardiovascular complication in metabolic disorders [7], and cancer [8]. Among the three NOS isoforms, iNOS is the most implicated in the development of different human malignant tumors, including those of the brain, head and neck, thyroid, breast, lung, stomach, pancreas, liver, colon [9].

Malignant gliomas, are aggressive brain tumors with limited therapeutic options and baleful prognosis. iNOS appears highly expressed in glioblastomas and grade III astrocytoma, with a positive correlation between iNOS expression and tumor grade [10]. In particular, iNOS appears to be a key regulator of malignant astrocytes transformations and of tumor cells proliferation. Therefore, it was suggested that iNOS inhibition might have potential therapeutic value in the treatment of gliomas.

Several iNOS inhibitors have been published to date, most of them targeting the arginine binding site of the enzyme oxygenase domain, which is highly conserved among the NOSs isoforms [11-13]. This makes the designof new selective iNOS inhibitors quite challenging, being an excellent degree of isoform selectivity, particularly over the eNOS, an essential requisite for a given iNOS inhibitor to avoid unwanted side effects. A major class of iNOS inhibitors are amidine derivatives, such as the aminoacidic derivative L-NIL, the cyclic amidine ONO-1714 and the aromatic acetamidine 1400W (Fig. 1) [14]. This latter is one of the most potent and selective iNOS inhibitors reported to date [15], although it never passed into clinical use.

(Figure 1 here as a single column image)

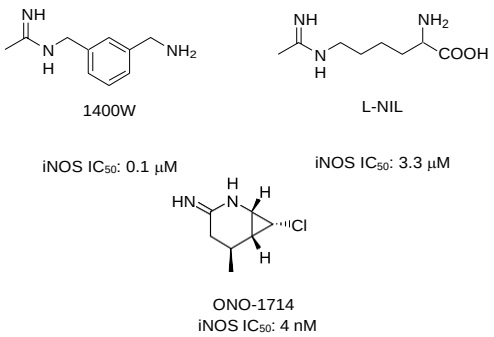

Fig. 1 Amidines inhibitors of iNOS

In our continuous effort to develop selective NOS inhibitors, we have published different acetamidines structurally related to the 1400W leading scaffold (Fig. 2) [16-19].

(Figure 2 here as a single column image)

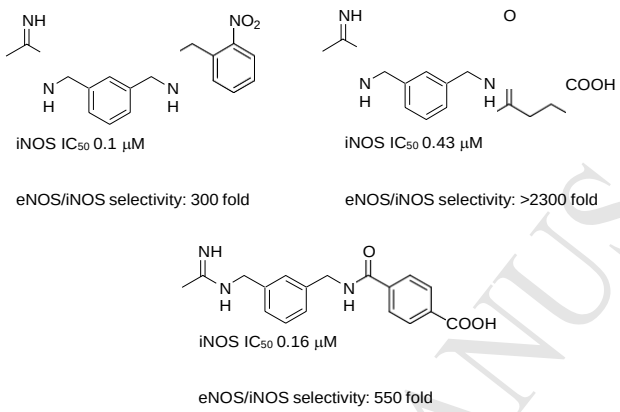

Fig.2 Acetamidines structurally related to 1400W

From these studies, it emerged that the substitution of the primary amino group of 1400W with lipophilic moieties containing ionizable groups was useful to give new selective iNOS inhibitors with improved selectivity over eNOS. Moreover, a molecular modeling study suggested that the introduction of a positively charged functional group in the molecular scaffold of a potential iNOS ligand, could be critical in conferring selectivity over eNOS [20]. Therefore, continuing the exploration of the structure-activity relationships of the N-[(3- aminomethyl)benzyl]-acetamidine scaffold, we have designed a new series 1400W derivatives, aiming to improve the isoform selectivity (**21-39**, Fig. 3). The molecular design was based on the potential favorable role that both hydrophobic and positively charged groups could have in the enzymatic recognition, particularly interacting with specific residues of the substrate access channel. Indeed, for example, L-NIL contains an L-Lys fragment and is a potent iNOS inhibitor. Therefore, the natural amino acids were chosen as substituents of the 3- aminomethyl tail of the 1400W scaffold. Gly was not included, as the corresponding derivative was previously reported [19].

(Figure 3 here as a 1.5 column image)

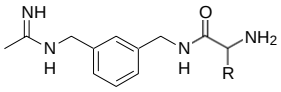

21-38

21: R=CH_3 (Ala); 22: R=  (Ile); 23: R=  (Leu); 24: R=  (Val); 25: R=  (Met);

26 R=  (Cys); 27 R=  (Ser); 28:R=  (Thr);29: R=  (Asn); 30: R=  (Gln);

31:R=  (Arg); 32 : R=  (His); 33: R=  (Phe); 34: R= (Lys);

35: R= (Asp); 36: R=  (Glu); 37: R=  (Tyr); 38: R=  (Trp)

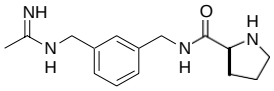

39

Fig.3. Chemical structures of target molecules

In this work, we describe the synthesis of compounds **21-39** and the *in vitro* evaluation against the NOSs.Moreover, as *N*-{3-[(ethanimidoylamino)methyl]benzyl}-L-prolinamide dihydrochloride (**39**) gave encouraging *in vitro* results, we discuss the promising findings obtained from an *ex vivo* evaluation of **39**, together with the biological effects on glioma cells line. Finally, results from a docking study performed on **39** are showed.

2. Results and discussion

2.1 Chemistry.

The syntheses of compounds **21-39** were performed according to Scheme 1. Compound 1 (1400W) was synthesized as previously reported [21], and then was coupled with the appropriate Boc-protected or Boc-(O-*t*Bu) protected amino acid, in the presence of isobutyl-chloroformate and NMM, to give intermediates **2-20**. The latter were treated with HCl in dioxane to remove the protecting groups, obtaining the desired compounds **21-39** ingood yields (70-97%) and excellent purity (>95%).

(Scheme 1 here as a 1.5 column image)

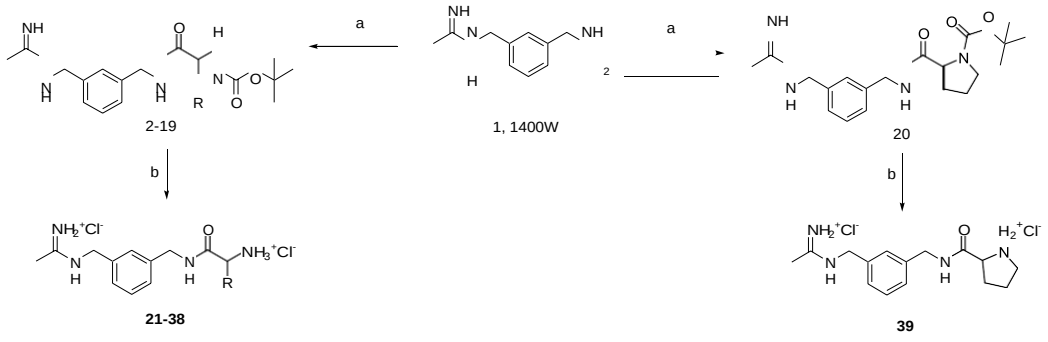

Scheme 1. Synthesis of target molecules 21-39. Reagents and conditions. a:Boc-protected or Boc(OtBu)- protected amino acid, iBuOCOCl, NMM, DMF dry, N_2, -15 °C to r.t. , 18-24h; b: HCl 4N, 1,4 dioxane, r.t., 24 h.

2.2 Nitric Oxide Synthases inhibition study.

As all the synthesized molecules are acetamidines virtually directed against iNOS, this isoform was at first assayed in the presence of compounds **21-39** by means of the radiometric ^{3}[H]- L-citrulline assay. Subsequently, compounds showing interesting iNOS inhibition (i.e. IC_{50}<10 μM), were further investigated against eNOS, to ascertain isoform selectivity. Indeed, eNOS plays a pivotal role in the vasculature and an excellent degree of selectivity over this isoform is an essential requisite for a given iNOS inhibitor. The obtained results, expressed as IC_{50} and isoform selectivity, are reported in Table 1. The substitution of the 1400W aminomethyl tail with the L- Ala, L-Ile and L-Leu residues (compounds **21-23**, respectively), gave potent iNOS inhibitors (IC_{50} =0.276 μM, 0.170 μM, and 0.253 μM, respectively), also showing an excellent degree of selectivity over eNOS. In particular, molecule **22**, albeit being less potent with respect to 1400W, gave a substantial improvement of isoform selectivity (>5850 folds). Similarly, compounds **31** and **32** bearing L-Arg and L-His, respectively, gave promising iNOS inhibition, with a submicromolar potency of action (IC_{50}= 0.450 μM and 0.534 μM, respectively) and excellent isoform selectivity.

Table 1. Inhibition of iNOS and eNOS by 21-39: IC_{50} ad Selectivity

Compd	IC_{50}[a] (μM)		Selectivity e/i
	iNOS	eNOS	
21	0.276±0.01	>1000	>3600
22	0.170±0.01	>1000	>5850
23	0.253±0.01	300	1183
24	>10	n.d.	-
25	>10	n.d.	-
26	>10	n.d.	-
27	>10	n.d.	-
28	>10	n.d.	-
29	>10	n.d.	-

30	>10	n.d.	-
31	0.450±0.03	>1000	>2220
32	0.534±0.02	>1000	>1873
33	>10	n.d.	-
34	0.446±0.02	211±17	473
35	1.025±0.04	331±20	323
36	1.229±0.06	10±0.8	8
37	>10	n.d.	-
38	>10	n.d.	-
39	0.058±0.005	265±21	4569
1400W	0.101±0.01	384±	3802

[a]Values given are mean ± SD of experiments performed in triplicate at seven different concentrations

However, **31-32** were not more active and selective than the reference compound. A significant decrease of the overall biological activity with respect to 1400W, was observed for molecules **34-36**. The best IC_{50} (0.446 μM)and e/i isoform selectivity degree (473 folds) were obtained from molecule **34**, bearing L-Lys residue, while molecules showing the acidic amino acids L-Asp and L-Glu (**35** and **36**, respectively) gave mild iNOS inhibition, with a drop of selectivity over eNOS for **36** (e/i ratio= 8 folds). Compounds **24-30**, **33**, and **37-38** resulted quite inactive against iNOS, therefore eNOS inhibition in the presence of these molecules was not evaluated. Significantly better results were obtained from compound **39**, bearing the L-Pro residue: it gave a potent iNOS inhibition (IC_{50}: 0.058 μM), with a selectivity of 4569 folds over eNOS. Based on this achievement, **39** emerged as the most interesting inhibitor of the series, producing a substantial improvement of both iNOS inhibition potency and selectivity with respect to the reference compound 1400W. Therefore, molecule **39** was selected for further investigations.

Initially, the neuronal NOS activity was evaluated in the presence of **39**, in order to exclude any potential interference with this isoform, which plays essential roles in the nervous system. As shown in Table 2, **39** did not inhibit nNOS (IC_{50} >10 μM), demonstrating a high i/n isoform selectivity degree, with a substantial improvement of this result with respect to 1400W (172 folds *vs* 77 folds).

Table 2. Inhibition of nNOS by 39: IC50 and Selectivity

Compd	IC_{50} [a] (μM)		Selectivity i/n
	nNOS	iNOS	
39	>10	0.058±0.005	>172
1400W	7.8±0.04	0.101±0.01	77

[a]Values given are mean ± SD of experiments performed in triplicate at seven different concentrations

2.3 *Ex vivo* selectivity of 39.

The iNOS selective inhibitory ability of **39** was evaluated in perfused mesenteric vessels isolated from rats treated *in vivo* with bacterial lipopolysaccharide (*E. coli* LPS, 30 mg kg -1, i.p.). The endotoxin-induced septic shock is characterized by hyporeactivity to noradrenaline (NA)-mediated vasoconstriction that largely depends on dysregulated production of NO generated by iNOS [22]. In mesenteric vessels from LPS-treated rats, administration of NA (10 nM – 10 μM) resulted in a dose-dependent increase in perfusion pressure, indicative of vessel contraction. Curves obtained in response to NA under basal conditions (CTRL) were repeated under incubation with **39** (0.06 μM/ 30 min). Subsequently, NA-dependent vasoconstriction was evaluated in the presence of N^{ω}-Nitro-L-arginine methyl ester (L-NAME, 100 μM/30 min), an arginine analog acting as non selective inhibitor of all NOS isoforms. With respect to NA dose-response obtained under basal conditions (CTRL curve), the maximal NA vasoconstriction (peak effect) was significantly increased in vessels pre- incubated with **39** (Fig. 4, panel A: $p < 0.05$ vs. each individual NA dose). As expected, and consistent with L- NAME ability to inhibit NO biosynthesis from all NOS isoforms, NA-mediated vasoconstriction was further enhanced under L-NAME incubation (Fig. 4, panel A: $p < 0.001$ *vs.* CTRL; $p < 0.01$ *vs.* compound **39**).Analogous results were obtained when the total extent of vasoconstriction induced by NA (AUC) was evaluated under basal conditions (CTRL), and compared to that obtained in the presence of compound **39** and in thepresence of L-NAME (Fig.4, panel B). Altogether, these findings support the selective inhibitory activity of **39** on iNOS toward eNOS isoforms under *ex vivo* conditions.

(Figure 4 here as a single column image)

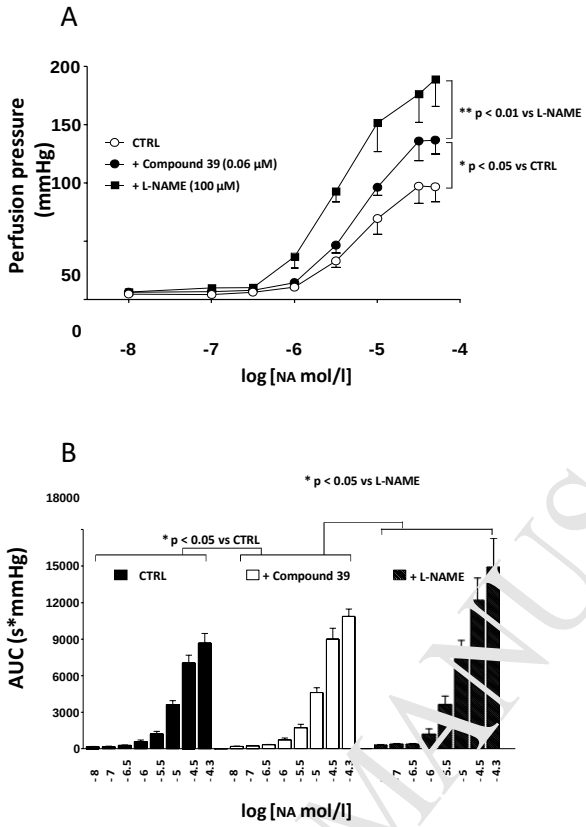

Fig.4. ***Ex vivo*** **evaluation of 39 effects on NA-mediated vasoconstriction.** Dose-response curves for NA- induced vasoconstriction (10 nM - 10 µM) were obtained in mesenteric vascular arteries (MVA) under basal conditions (CTRL), after pre-treatment with 39 and after subsequent treatment with L-NAME. Panel A. Maximal vasoconstriction to individual NA doses (peak ef-fect) was measured as perfusion pressure value and expressed in mmHg. Panel B. Duration of vasoconstriction obtained with individual NA doses (10 nM - 10 µM) was calculated as area under the curve (AUC) and expressed as perfusion pressure (mmHg) x time (sec). Results are mean ± SEM of duplicates from 4 experiments independently repeated.

2.4 Cell metabolic activity of rat astrocytes and C6 rat glioma cell line towards 39.

In order to evaluate the biological activity and the selectivity of **39**, the MTT (3-(4,5-dimethylthiazol-2-yl)-2,5-diphenyltetrazolium bromide) test was performed on both CTX/TNA2 rat normal astrocytes and their pathological counterpart, C6 rat glioma cells. As element of comparison, 1400W was also tested on both cell lines in the same range of concentrations. Fig. 5a shows the percentage of metabolic activity of CTX/TNA2 rat astrocytes after a 24, 48 and 72 h administration of **39** and 1400W (0-2 mM). As regards 1400W (Fig. 5a, right panel), a reduction of cell metabolic activity was clearly detected after 24 h with the lowest tested concentration (0.25 mM). Increasing concentrations of 1400 W further lowered CTX/TNA2 metabolic activity in a dose- dependent manner.

(Figure 5 here as a double column image)

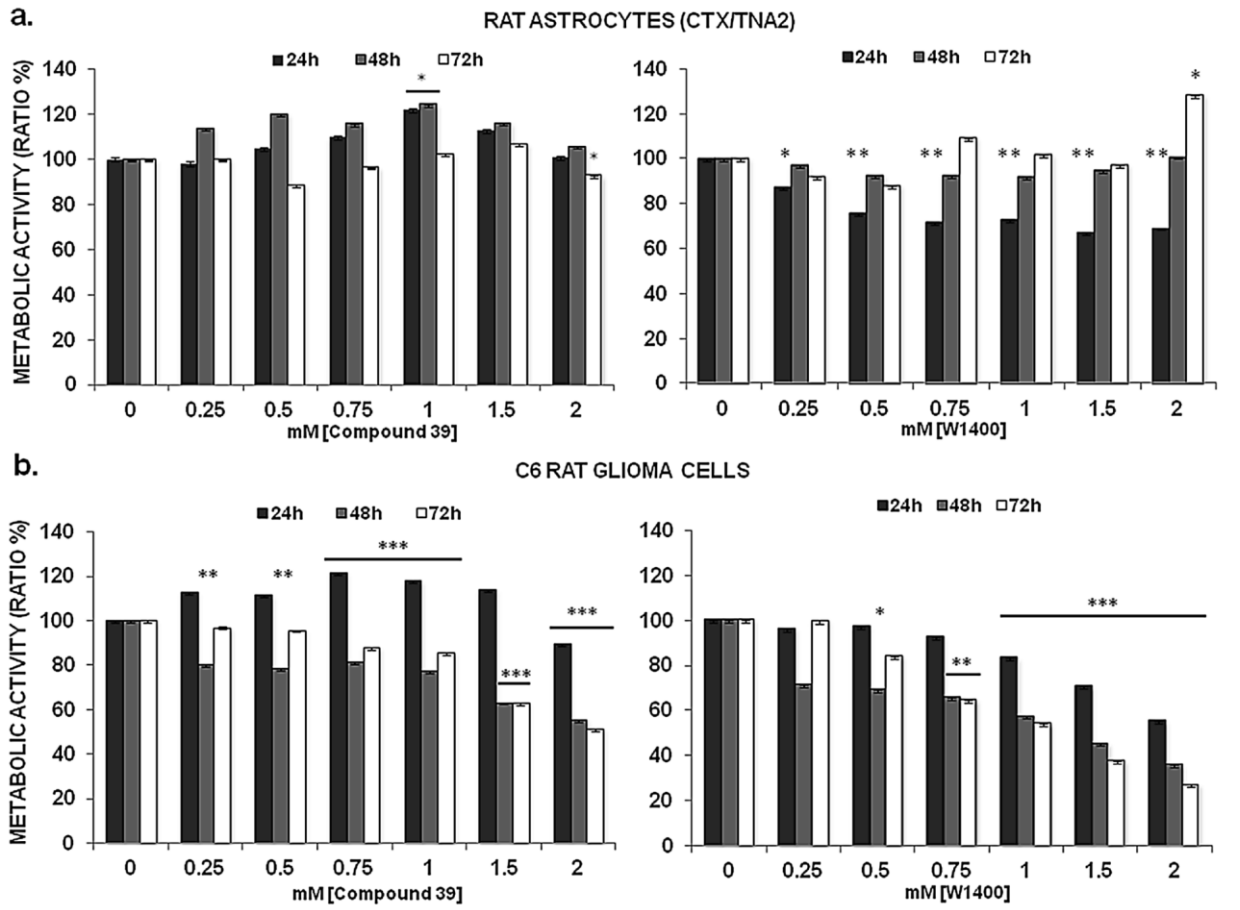

Fig.5. Cell metabolic activity of CTX/TNA2 rat astrocytes and C6 rat glioma cells exposed to loading concentrations of 39. Metabolic activity of rat astrocytes (a) and C6 rat glioma cells (b) expressed as the ratio (%) of the untreated cells (0 mM compound **39** or 1400W) measured by the MTT test. Results represent themeans ± SD (n=9). *p<0.05, **p<0.01, ***p<0.001 cells treated vs untreated cells.

Notably, a 24 h exposure to 1.5 mM and 2 mM 1400W significantly (p<0.01) dropped cell metabolic activity up to 67.36% and 69.18%, respectively. The inhibition of cell proliferation by 1400 W was not reproducible over the exposure time, being not detectable after 48 and 72 h, when the percentage of cell metabolic activity reverted to the ones of untreated cells. Quite the opposite, compound **39** (Fig. 5a, left panel) exerted no significant effects on the proliferation of rat astrocytes. Indeed, the cell metabolic activity slightly increased after 24 and 48 h with **39**, starting from 0.5 mM, and being significantly raised with 1 mM of **39** (121.93 % after 24 h and 124.56% after 48 h). In the second group of assays, the same experimental set up was applied on C6 rat glioma cells. (Fig. 5b). As

regards 1400 W, the percentage of the metabolic activity of glioma cells clearly decreased after 24 h in a dose-dependent mode, being significantly ($p<0.001$) reduced in the presence of 1, 1.5 and 2 mM 1400 W (83.20%, 70.60% and 55.17%, respectively). After 48 h, the dose-dependent inhibition of cell proliferation was detectable from lower concentrations than 1 mM, starting from 0.5 mM 1400W (68.94%) up to 2 mM 1400W (35.66%). The significant ($p<0.01$) inhibition of cell proliferation was maintained also after 72 h of exposure, being the percentage of cell metabolic activity around 64.61% after the administration of 0.75 mM 1400 W (Fig. 5b, left panel). By contrast, after a 24 h administration of **39** to C6 rat glioma cells, the percentage of cell metabolic activity increased, being significantly ($p<0.01$) augmented in the presence of 1 mM and 1.5 mM of **39** (118.00% and 114.17%, respectively). After these concentrations, the percentage of active cells slightly decreased up to 89.51% after the administration of 2 mM of **39**. Quite the opposite, a 48 h administration of **39** clearly decreased the percentage of active metabolizing cells, starting from the lowest concentration of 0.25 mM (80.42%). The inhibition of cell proliferation was even more significant ($p<0.001$) and dose-dependent in the presence of higher concentrations of **39** (0.75-2 mM), being 77.45% at 1 mM, 63.25% at 1.5 mM and 55.25% at 2 mM. The slowdown of the proliferation rate was maintained after a 72h exposure being even more exacerbated with the highest concentrations of **39** (Fig. 5b, left panel).

These data are in accordance with selectivity data from the radiometric ^{3}[H]- L-citrulline assay, being **39** not effective on CTX/TNA2 rat astrocytes while it was found significantly active on C6 rat glioma cells. Indeed, the inducible isoform of NOS is not expressed under physiological conditions, therefore **39** seems not able to bind its molecular target inside astrocytes and to exert its pharmacological activities. On the contrary, **39** was found notably active on C6 rat glioma which overexpressed iNOS as a marker of malignancy. The rise of the cell metabolic activity after 24 h of administration of **39** on glioma cells may be due to mechanisms of chemoresistence active in malignat gliomas [23], and further investigations are needed to demonstrate the implications at the molecular level. Furthermore 1400W exerted an inhibitory effect on normal astrocytes after 24
h. It is quite plausible to assume that 1400W acts also on the constitutive isoforms of NOS, confirming once again selectivity data of the radiometric ^{3}[H]- L-citrulline assay.

2.5 Cytotoxicity of 39 on C6 rat glioma cells.

Cytotoxicity occurrence was assessed using the CytoTox 96® Non-Radioactive Cytotoxicity Assay which measures lactate dehydrogenase (LDH), a stable cytosolic enzyme that is released upon cell lysis and thus evincive of cell necrosis. The percentages of LDH released in cell supernatants after 24, 48 and 72 h of exposure to **39** are reported in Fig. 6, left panel. In spite of no evident fluctuations at early stages, **39** exerted a significant ($p<0.01$) cytotoxic effect after 72 h of exposure starting from 0.25 and 0.5 mM (26.54 % and 27.21%, respectively) with respect to untreated cells (5.41 %). After these concentrations, the percentage of LDH fell down, assessed at 20.99% with 0.75 mM, 16.78 with 1 mM and 23.27 % with 1.5 mM. The exposure to 2 mM of compound 39 clearly raised LDH release up to 25.52 %.

2.6 Cell cycle progression and G1 arrest of C6 rat glioma cells exposed to 39.

To better understand proliferation data from the MTT assay and whether **39** could activate checkpoints resulting in cell cycle arrest as a response to iNOS inhibition, cell cycle progression was analyzed after 72 h of exposure by means of flow cytometry. Untreated C6 rat glioma cells were found active and proliferating, with 63.97% of cells in phase G1 and 22.64% of cells undergoing phase S (Fig. 6, right panel). Although not dose-dependent, a shrinking of phase S and an increase of phase G1 were found in the presence of **39**, being significantly evident ($p<0.01$) with 1.5 mM (12.12% phase S and 71.79% phase G1). These data suggest that **39** inhibits cell proliferation, arresting cell cycle at the G1/S phase checkpoint.

(Figure 6 here as a single column image)

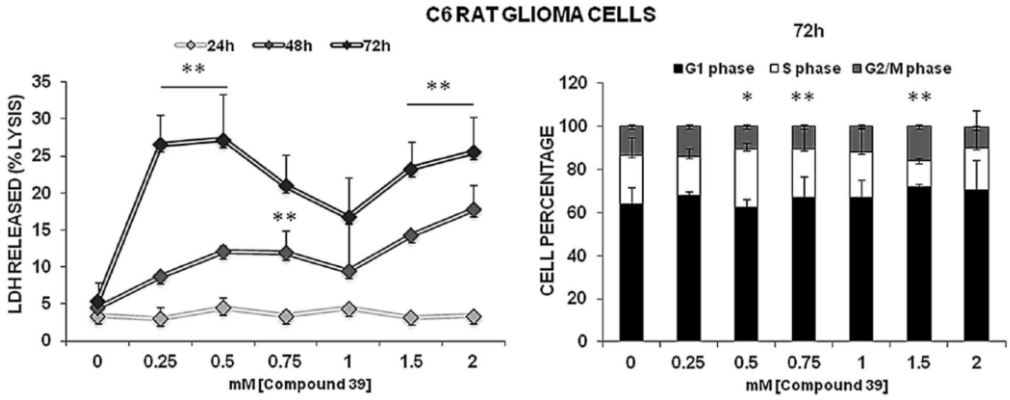

Fig.6. Cytotoxicity and cell cycle progression of loading concentrations of 39 on C6 rat glioma cells. Left panel: cytotoxicity occurrence measured by the percentage of lactate dehydrogenase released from C6 rat glioma cells after 24-72 h of exposure to loading concentrations of **39**. Right panel: cell cycle progression of C6 rat glioma cells treated with increasing concentrations of compound **39** after 72h. Results represent the means ± SD (n=9). *$p<0.05$, **$p<0.01$ cells treated *vs* untreated cells.

2.7 Docking Studies.

To shed some light on the structural basis for the evaluated potency and selectivity, a molecular docking study of the most active compound with a proline group on the 3-aminomethyl tail of the 1400W scaffold, **39,** into eNOS and iNOS binding sites was performed. Docking results showed for the pose of **39** into the binding site of iNOS the same interactions observed for 1400W, i.e. between the acetamidine moiety and a GLU and a TRP residues of the iNOS binding site and between the amide N-H group and one of the heme propionate arm, plus a further hydrogen bond between the proline amino group and the remaining propionate arm (Fig. 7). On the other hand, the results for the docking of **39** into the binding site of eNOS showed, beyond the standard interactions between

the acetamidine moiety and the GLU and TRP residues, only a hydrogen bond of the proline amino group with one of the heme propionate arm, while the linking amide formed weak hydrogen bonds interactions with the same propionate arm from one side and an arginine residue of the binding pocket on the other side (see Fig. S.1 in Supplementary data).

(Figure 7 here as a single column image)

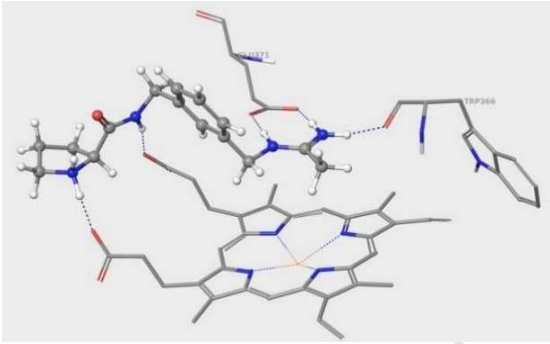

Fig.7. Interactions responsible for the binding of **39** into the binding site of iNOS.

3. Conclusions

A new series of acetamidine based compounds as selective iNOS inhibitors was synthesized. Different molecules gave a potent iNOS inhibition, with an improved isoform selectivity compared to the reference compound 1400W. Among these molecules, **39** was the most potent and selective one, and confirmed its isoform selectivityon rats mesenteric vessels, in *ex vivo* conditions. Our docking study shed light on the critical role of the proline moiety of **39** in conferring iNOS selectivity. Finally, exposition to **39** of C6 rat glioma cells, gave encouraging results, since this molecule was cytotoxic and antiproliferative, arresting cell cycle at the G1/S phase checkpoint, with no detectable effects on rat normal astrocytes. Therefore, based on the obtained preliminary results, **39** emerges as a promising molecular tool for the therapy of malignant glioma.

4. Experimental Protocols

4.1 Chemistry

4.1.1 General methods and materials

All chemicals were purchased from commercial sources and used without further purification. Flash chromatography was performed on silica gel 60 (Merck) and TLC on silica gel 60, F254. Infrared spectra were recorded on a FT-IR 1600 Perkin-Elmer spectrometer. Melting points were determined on a Buchi apparatus and

given uncorrected. NMR spectra were run on a Varian instrument, operating at 300 (^{1}H) or 75 (^{13}C) MHz; chemical shifts (δ) are reported in ppm. HPLC analyses were performed using a Waters (Milford, MA, USA) system composed of a P600 model pump, a 2996 photodiode array detector, and a 7725i model sample injector (Rheodyne, Cotati, CA, USA). Chromatograms were recorded on a Fujitsu Siemens Esprimo computer and the Empower Pro software (Waters) processed data. The analyses were performed on an XTerra MS C8 column (250 x 4.6 mm id, 5 μm particle size) (Waters), equipped with an XTerra MS C8 guard column (Waters). A column thermostat oven module Igloo-Cil (Cil Cluzeau Info Labo, France) was used. To evaluate target compounds purity, the column was eluted at a flow rate of 1 mL/min with a mixture of 8 mM sodium borate (pH = 10) and CH_3OH (mobile phase composition ranging from 50/50 to 75/25). All tested compounds had a purity of ≥95%. Mass spectra were obtained on a Thermofinnigan LCQ Advantage spectrometer (ESI). Elemental analyses were carried out by a Eurovector Euro EA 3000 model analyzer. Analyses indicated by the symbols of the elementswere within ± 0.4% of the theoretical values.

4.1.2 Generic synthesis of compounds 2-20

The appropriate ter-butoxycarbonyl, ter-butyl or ter-butoxy full protected amino acid (0.002 mol) was dissolved in dry DMF (4 mL) and NMM (0.002 mol) was added under N_2. After 5 minutes under stirring at -10 °C, isobutylchloroformate was added (0.002 mol) and the mixture reacted for 10 minutes. Then a solution of 1400W (0.0025 mol) in dry DMF (3 mL) was added, and after 20 h at 0 °C and 4 h at room temperature, reaction were quenched with water. The solvent was removed under reduced pressure, and the crude product was purified by column chromatography on silica gel (CH_2Cl_2/ CH_3OH, 9:1) or by semipreparative HPLC (Polarity C18 column, H_2O/CH_3CN 70:30 with 0.1% v/v of TFA).

1-{[3-({[N-(tert-butoxycarbonyl)-L-alanyl]amino}methyl)benzyl]amino}ethaniminium chloride (**2**)

Hygroscopic white solid, 54% yield. ^{1}HNMR (300 MHz, CD_3OD) δ: 1.32 (d, J=7.2 Hz, 3H, CH_3), 1.42 (s, 9H, CH_3), 2.25 (s, 3H, CH_3), 4.06 (q, J= 6.3 Hz, 1H, CH), 4.32-4.46 (m, 4H, CH_2), 7.22-7.35 (m, 4H, CHAr), 8.36 (bs, 1H, NH), 8.77 (bs, 1H, NH), 9.21 (bs, 1H, NH), 9.81 (bs, 1H, NH); ^{13}CNMR (75 MHz, CD_3OD) δ: 17.1, 17.7, 27.5, 42.4, 46.0, 53.6, 79.4, 127.1, 129.0, 134.7, 139.8, 156.5, 164.9, 175.1. MS (ESI): m/z (%): 349.4(100) [M+H$^+$];

1-{[3-({[N-(tert-butoxycarbonyl)-L-isoleucyl]amino}methyl)benzyl]amino}ethaniminium chloride (**3**)

Hygroscopic white solid, 40% yield. ^{1}HNMR (300 MHz, CD_3OD) δ: 0.91(t, J= 6.9 Hz, 6H, CH_3), 1.10 (septet, J=7.5 Hz, 1H, CH), 1.43 (s, 9H, CH_3), 1.88-1.92 (m, 1H, CH), 2.27 (s, 3H, CH_3), 3.90 (d, J=7.2 Hz, 1H, CH), 4.33-4.45 (m, 4H, CH_2), 7.23-7.38 (m, 4H, CHAr), 8.59 (bs, 1H, NH); ^{13}CNMR (75 MHz, CD_3OD) δ: 10.3, 14.8, 17.7, 24.7, 27.5, 36.9, 42.5, 46.0, 59.8, 79.4, 126.6, 129.0, 134.6, 139.4, 139.8, 157.8, 164.9, 173.6. MS (ESI): m/z (%): 391.5(100) [M+H$^+$]

1-{[3-({[N-(tert-butoxycarbonyl)-L-leucyl]amino}methyl)benzyl]amino}ethaniminium chloride (**4**)

Hygroscopic white solid, 30% yield. ^{1}HNMR (300 MHz, CD_3OD) δ: 0.98 (d, J=6.3 Hz, 6H, CH_3), 1.42 (s, 9H, CH_3), 1.55 (t, J= 7.2 Hz, 2H, CH_2), 1.68 (m, 1H, CH), 2.25 (s, 3H, CH_3), 4.10 (q, J= 7.2 Hz, 1H, CH), 4.32-4.43 (m, 4H, CH_2), 7.23-7.37 (m, 4H, CHAr), 7.96 (bs, 1H, NH); ^{13}CNMR (75 MHz, CD_3OD) δ: 17.7, 22.2, 24.7, 27.5, 40.6, 42.9, 46.9, 53.7, 79.4, 126.5, 126.9, 127.1, 129.0, 134.6, 139.8, 164.7, 174.9. MS (ESI): m/z (%): 391.5(100) [$M+H^+$]

1-{[3-({[N-(tert-butoxycarbonyl)-L-valyl]amino}methyl)benzyl]amino}ethaniminium chloride (**5**)

Hygroscopic white solid, 35% yield ^{1}HNMR (300 MHz, CD_3OD) δ: 0.93 (d, J= 6.6 Hz, 6H, CH_3), 1.43 (s, 9H, CH_3), 2.03 (q, J=6.9, 1H, CH), 2.25 (s, 3H, CH_3), 3.83 (t, J=6.9 Hz, 1H, CH), 4.38-4.45 (m, 4H, CH_2), 7.22-7.38 (m, 4H, CHAr); 8.55 (bs, 1H, NH); ^{13}CNMR (75 MHz, CD_3OD) δ: 17.3, 17.7, 18.6, 27.5, 30.6, 42.5, 46.0, 60.8, 79.4,126.6, 127.0, 127.3, 129.0, 134.7, 139.8, 156.8, 164.9, 173.5. MS (ESI): m/z (%): 377.26 (100) [$M+H^+$]

1-{[3-({[N-(tert-butoxycarbonyl)-L-methionyl]amino}methyl)benzyl]amino}ethaniminium chloride (**6**)

Hygroscopic yellow solid, 25% yield; ^{1}HNMR (300 MHz, DMSO) δ: 1.36 (s, 9H, CH_3), 1.82 (septet, J= 7.2 Hz, 2H, CH_2), 2.05 (s, 3H, CH_3), 2.17 (s, 3H, CH_3), 2.39-4.44 (m, 2H, CH_2), 4.01 (q, J= 5.1 Hz, 1H, CH), 4.26 (d, J=4.2 Hz, 2H, CH_2), 4.38 (d, J=5.7 Hz, 2H, CH_2), 7.02-7.32 (m, 4H, CHAr), 8.38 (bs, 2H, NH), 8.70 (bs, 1H, NH), 9.14 (bs, 1H, NH), 9.74 (bs, 1H, NH); ^{13}CNMR (75 MHz, DMSO): δ 15.3, 19.4, 28.8, 30.4, 32.1, 42.5, 45.9, 54.3, 78.8, 126.8, 127.1, 127.2, 129.3, 135.6, 140.8, 156.1, 164.9, 172.6. MS (ESI): m/z (%): 409.2 (100) [$M+H^+$];

1-{[3-({[N-(tert-butoxycarbonyl)-L-cysteyl]amino}methyl)benzyl]amino}ethaniminium chloride (**7**)

Hygroscopic yellow solid, 21% yield; ^{1}HNMR (300 MHz, DMSO) δ: 1.44 (s, 9H, CH_3), 2.27 (s, 3H, CH_3), 3.73 (s, 2H, CH_2), 3.87 (q, J=5.2 Hz, 1H, CH), 4.40 (s, 2H, CH_2), 4.44 (s, 2H, CH_2), 7.23-7.38 (m, 4H, CHAr); ^{13}CNMR (75 MHz, DMSO): δ 17.8, 27.5, 42.4, 43.5, 46.0, 54.39, 79.6, 126.8, 126.6, 126.8, 127.2, 129.0, 134.7, 139.8, 157.3, 164.9, 171.6. MS (ESI): m/z (%): 381.2 (100) [M+H+];

1-{[3-({[N-(tert-butoxycarbonyl)-O-(tert-butyl)-L-seryl]amino}methyl)benzyl]amino}ethaniminium chloride (**8**)

Yellow sticky solid, 47% yield; ^{1}HNMR (300 MHz, DMSO) δ 1.07 (s, 9H, CH_3), 1.36 (s, 9H, CH_3), 2.16 (s, 3H, CH_3), 3.45 (dd, J=5.4Hz, 2.4Hz, 2H, CH_2), 4.03 (q, J=5.7 Hz, 1H, CH), 4.28 (dd, J= 10.2 Hz, 6.0 Hz, 2H, CH_2), 4.37 (s, 2H, CH_2), 7.17-7.35 (m, 4H, CHAr), 8.38 (t, J=6.0 Hz, 1H, NH), 8.65 (bs, 1H, NH), 9.17 (bs, 1H, NH), 9.76 (bs, 1H, NH). ^{13}CNMR (75 MHz, DMSO) δ 19.4, 27.8, 28.7, 42.5, 45.9, 55.7, 62.5, 67.9, 73.4, 78.9, 126.8, 127.1, 127.2, 129.2, 135.5, 140.7, 155.8, 164.9, 170.9. MS (ESI): m/z (%): 421.2(100) [M+H+];

1-{[3-({[N-(tert-butoxycarbonyl)-O-(tert-butyl)-L-threonyl]amino}methyl)benzyl]amino}ethaniminium chloride (**9**)

Yellow oil, 30% yield; ^{1}HNMR (300 MHz, DMSO) δ 0.99 (d, J= 5.8 Hz, 3H, CH_3), 1.06 (s, 9H, CH_3), 1.37 (s, 9H, CH_3), 2.16 (s, 3H, CH_3), 3.86-3.91 (m, 2H, CH), 4.20-4.37 (m, 4H, CH_2), 7.17-7.35 (m, 4H, CHAr), 8.28 (t,

J=6.0 Hz, 1H, NH). ^{13}CNMR (75 MHz, DMSO) δ 19.4, 20.6, 28.7, 42.7, 45.9, 60.2, 67.9, 74.1, 79.1, 126.9, 127.4, 129.3, 135.6, 140.4, 155.8, 164.9, 170.8. MS (ESI): m/z (%): 435.5(100) [M+H+];

1-{[3-({[N^2,N^4-bis(tert-butoxycarbonyl)-L-asparaginyl]amino}methyl)benzyl]amino}ethaniminium chloride (**10**)

Hygroscopic white solid, 45% yield. ^{1}HNMR (300 MHz, CD_3OD) δ: 1.36 (s, 9H, CH_3), 1.56 (s, 9H, CH_3), 2.18 (s, 3H, CH_3), 3.14-3.33 (m, 2H, CH_2), 3.75 (q, J=5.4 Hz, 1H, CH), 4.26 (d, J=5.7 Hz, 2H, CH_2), 4.40 (s, 2H, CH_2), 7.15-7.32 (m, 4H, CHAr); 8.35 (t, J=5.7, 1H, NH); ^{13}CNMR (75 MHz, CD_3OD) δ: 19.3, 22.0, 28.4, 28.8, 42.5, 45.8, 52.1, 78.9, 79.4, 119.6, 126.9, 127.3, 129.2, 135.7, 140.7, 155.8, 156.8, 164.8, 171.5, 172.2. MS (ESI): m/z (%): 492.2(100) [M+H+]

1-{[3-({[N^2,N^5-bis(tert-butoxycarbonyl)-L-glutaminyl]amino}methyl)benzyl]amino}ethaniminium chloride (**11**)

Hygroscopic white solid, 42% yield. ^{1}HNMR (300 MHz, CD_3OD) δ: 1.32 (s, 9H, CH_3), 1.55 (s, 9H, CH_3), 1.70-1.98 (m, 2H, CH_2), 2.11 (q, J=6.9 Hz, 2H, CH_2), 2.17 (s, 3H, CH_3), 3.97 (q, J=4.5 Hz, 1H, CH), 4.28 (d, J=5.1 Hz, 2H, CH_2), 4.42 (s, 2H, CH_2), 7.18-7.4 (m, 4H, CHAr), 8.51 (t, J=6.0 Hz, 1H, NH); ^{13}CNMR (75 MHz, CD_3OD) δ: 19.4, 27.9, 28.3, 28.7, 38.9, 42.5, 46.9, 54.1, 79.5, 88.2, 127.7, 131.1, 131.9, 135.7, 139.4, 141.2, 150.4, 151.8, 155.7,162.3,168.7. MS (ESI): m/z (%): 506.3(100) [M+H+]

N^2-(tertbutoxycarbonyl) -N^5-{[(tertbutoxycarbonyl) amino] [(tertbutoxycarbonyl)-N^1-{3-[(ethanimidoylamino) methyl] benzyl}-L-argininamide (**12**)

Hygroscopic white solid, 50% yield. ^{1}H NMR (300 MHz, CD_3OD): δ 1.43 (s, 9H, CH_3), 1.46 (s, 9H, CH_3), 1.54 (s, 9H, CH_3), 1.63-1.74 (m, 4H, CH_2), 2.26 (s, 3H, CH_3), 3.79-3.90 (m, 2H, CH_2), 4.03 (t, J=6.3 Hz, 1H, CH), 4.34-4.46 (m, 4H, CH_2), 7.22-7.38 (m, 4H, CHAr); ^{13}C NMR (75 MHz, CD_3OD): δ 17.7, 25.2 27.0, 27.3, 27.5, 29.0, 42.5, 44.2, 46.0, 55.0, 78.8, 79.4, 84.0, 126.5, 126.9, 127.1, 129.0, 134.6, 139.8, 154.8, 156.71, 161.4, 165.0, 168.8, 174.1. MS (ESI): m/z (%): 634.39 (100) [M+H+]

1-{[3-({[N^3-bis(tert-butoxycarbonyl)-L-histidyl]amino}methyl)benzyl]amino}ethaniminium chloride (**13**)

Hygroscopic white solid, 41% yield. ^{1}HNMR (300 MHz, CD_3OD) δ: 1.31 (s, 9H, CH_3), 1.45 (s, 9H, CH_3), 2.17 (s, 3H, CH_3), 2.94-3.20 (m, 2H, CH_2), 4.44 (d, J= 5.2 Hz, 2H, CH_2), 4.76 (q, J=5.4 Hz, 1H, CH), 4.86 (s, 2H, CH_2), 6.96-7.31 (m, 4H, CHAr), 6.99 (d, J=6.0 Hz, 1H, CHAr), 7.63 (s, 1H, CHAr), 8.37 (t, J=6.0 Hz, 1H, NH) ; ^{13}CNMR (75 MHz, CD_3OD) δ: 17.4, 28.3, 29.5, 30.4, 41.9, 46.9, 55.4, 79.4, 85.2, 114.7, 126.6, 127.7, 131.0, 131.8, 135.7, 139.3, 142.0, 141.0, 151.8, 155.7, 162.3, 168.7. MS (ESI): m/z (%): 515.3 (100) [M+H+]

1-{[3-({[N-(tert-butoxycarbonyl)-L-phenylalanyl]amino}methyl)benzyl]amino}ethaniminium chloride (**14**)

White solid, 37% yield; mp 99-102°C; ^{1}HNMR (300 MHz, DMSO): δ 1.28 (s, 9H, CH_3), 2.16 (s, 3H, CH_3), 2.75 (m, 1H, *H*CH), 2.95 (dd, J=13.8 Hz, 5.1 Hz, 1H, HC*H*), 4.17 (sextet, J= 3.6 Hz, 1H, CH), 4.28 (d, J=5.7 Hz, 2H, CH_2), 4.39 d, J=6.0 Hz, 2H, CH_2), 7.00-7.33 (m, 9H, CHAr), 8.48 (t, J=6.0, 1H, NH), 8.70 (bs, 1H, NH), 9.15 (bs,

1H, NH), 9.75 (bs, 1H, NH); ^{13}C NMR (75 MHz, DMSO): δ 19.4, 28.8, 38.1, 42.5, 45.9, 56.6, 78.7, 126.8, 127.1, 127.8, 128.7, 129.3, 129.8, 135.6, 138.8, 140.7, 155.9, 164.9, 172.4. MS (ESI): m/z (%): 425.3(100) [M+H+];

N^2, N^6-bis (tert-butoxycarbonyl) –N^1- {3-[(ethanimidoylamino) methyl] benzyl}-L-lisinamide (**15**)

Hygroscopic white solid, 40% yield. ^{1}HNMR (300 MHz, CD_3OD): δ 1.43 (s, 18H, CH_3), 1.59-1.65 (m, 2H, CH_2), 1.70-1.75 (m, 2H, CH_2), 2.26 (s, 3H, CH_3), 3.02 (q, J=6.6 Hz, 4H, CH_2), 3.99 (q, J=5.1 Hz, 1H, CH), 4.32-4.46 (m, 4H, CH_2), 7.23-7.40 (m, 4H, CHAr); ^{13}CNMR (75 MHz, CD_3OD): δ 17.7, 23.0, 27.5, 27.6, 29.4, 31.7, 39.7, 42.5, 46.0, 55.2, 78.7, 79.4, 126.5, 126.9, 127.2, 129.0, 134.6, 139.9, 156.7, 157.4, 164.9, 174.4. MS (ESI): m/z (%): 506.3(100) [M+H+]

tert-butyl N^2-(tert-butoxycarbonyl)-N^1-{3-[(ethanimidoylamino)methyl]benzyl}-L-aspartate hydrochloride (**16**)

Hygroscopic white solid, 30% yield. : ^{1}HNMR (300 MHz, DMSO) δ 1.35 (s, 9H, CH_3), 1.39 (s, 9H, CH_3), 2.17 (s, 3H, CH_3), 2.79 (t, J=6.0 Hz, 2H, CH_2), 4.17 (q, J= 5.3, 1H, CH), 4.24-4.38 (m, 4H, CH_2), 7.09-7.39 (m, 4H, CHAr); 8.37 (bs, 1H, NH), 8.78 (bs, 1H, NH), 9.18 (bs, 1H, NH), 9.75 (bs, 1H, NH); ^{13}CNMR (75 MHz, DMSO) δ: 19.3, 27.6, 28.5, 38.9, 44.3, 50.6, 52.2, 77.4, 82.6, 129.3, 132.3, 133.7, 133.9, 139.6 145.2, 159.7, 167.1, 169.8, 171.2. MS (ESI): m/z (%): 449.3 (100) [M+H+];

tert-butyl N^2-(tert-butoxycarbonyl)-N^1-{3-[(ethanimidoylamino)methyl]benzyl}-L-glutaminate hydrochloride (**17**)

Hygroscopic white solid, 45% yield; ^{1}HNMR (300 MHz, DMSO) δ 1.37 (s, 18H, CH_3), 1.68 (sextet, J= 4.5 Hz, 1H, *H*CH), 1.83 (sextet, J= 5.4 Hz, 1H, HC*H*), 2.16 (s, 3H, CH_3), 2.20 (t, J=7.5 Hz, 2H, CH_2), 3.91 (sextet, J=5.7 Hz, 1H, CH), 4.27 (d, J=6.0 Hz, 2H, CH_2), 4.38 (d, J=5.7, 2H, CH_2), 6.94-7.34 (m, 4H, CHAr), 8.36 (t, J=5.7, 1H, NH), 8.64 (s, 1H, NH), 9.18 (s, 1H, NH), 9.79 (bs, 1H, NH);^{13}CNMR (75 MHz, DMSO) δ 19.4, 27.7, 28.4, 28.8, 32.0, 42.5, 45.9, 54.3, 78.8, 80.3, 126.8, 127.11, 127.2, 129.3, 135.6, 140.8, 156.0, 164.9, 172.3, 172.4. MS (ESI): m/z (%): 463.5 (100) [M+H+];

1-{[3-({[N-(tert-butoxycarbonyl)-O-(tert-butyl)-L-tyrosyl]amino}methyl)benzyl]amino}ethaniminium chloride (**18**)

Hygroscopic white solid, 47% yield; ^{1}HNMR (300 MHz, DMSO) δ 1.23 (s, 9H, CH_3), 1.27 (s, 9H, CH_3), 2.16 (s, 3H, CH_3), 2.46-2.49 (m, 2H, CH_2), 4.11-4.19 (m, 1H, CH), 4.27 (d, J=6.0 Hz, 2H, CH_2), 4.39 (d, J=4.2 Hz, 2H, CH_2), 6.85 (d, J=8.4 Hz, 2H, CHAr), 6.99 (d, J=8.4 Hz, 1H, CHAr), 7.12-7.17 (m, 4H, CHAr), 7.28-7.33 (m, 1H, CHAr), 8.42 (t, J=6.0, 1H, NH), 8.63 (s, 1H, NH), 9.12 (s, 1H, NH), 9.77 (bs, 1H, NH);. ^{13}CNMR : (75 MHz, DMSO) δ 19.7, 28.2, 28.6, 39.8, 42.7, 45.8, 54.3, 77.6, 78.7, 114.1, 122.8, 126.2, 127.5, 130.5, 134.1, 134.9, 139.8, 140.0, 142.1, 147.9, 155.0, 169.0, 171.3. MS (ESI): m/z (%): 497.3(100) [M+H+];

1-{[3-({[N-(tert-butoxycarbonyl)-L-tryptophyl]amino}methyl)benzyl]amino}ethaniminium chloride (**19**)

Hygroscopic white solid, 40% yield; ^{1}HNMR (300 MHz, CD_3OD) δ: 1.37 (s, 9H, CH_3), 2.23 (s, 3H, CH_3), 3.06 (t, J=7.2 Hz, 2H, CH_2), 4.26 (d, J=4.2 Hz, 1H, CH), 4.33-4.37 (m, 4H, CH_2), 6.98-7.36 (m, 8H, CHAr), 7.60 (d, J=7.8 Hz, 1H, CHAr), 8.35 (bs, 1H, NH), 8.58 (bs,1H, NH), 9.10 (bs, 1H, NH), 9.26 (bs, 1H, NH), 9.81 (bs,1H, NH); ^{13}CNMR (75 MHz, CD_3OD) δ: 17.7, 27.4, 42.6, 42.7, 46.9, 53.4, 79.5, 109.7, 111.1, 118.2, 118.6, 121.2, 123.5, 126.5, 126.8, 127.1, 127.6, 129.0, 134.5, 136.9, 139.5, 161.7, 164.9, 173.8. MS (ESI): m/z (%): 464.2 (100) [M+H+];

1-{[3-({[1-(tert-butoxycarbon-yl)-L-prolyl]amino}methyl)benzyl]amino}ethaniminium chloride (**20**).

Hygroscopic pale yellow solid, 45 % yield; IR (KBr): 3416, 3279, 1681 cm^{-1}. ^{1}HNMR (300 MHz, CD_3OD): δ 1.26 (s, 9H, CH_3), 1.81-1.99 (m, 4H, CH_2), 2.17 (s, 3H,CH_3), 3.39-3.57 (m, 2H, CH_2), 4.11-4.38 (m, 3H, CH and CH_2), 4.41 (s, 2H, CH_2), 7.10-7.67 (m, 4H, Ar), 8.39 (bs, 1H, NH); ^{13}CNMR (75 MHz, CD_3OD) δ : 19.4, 23.9, 24.1, 28.6, 39.3, 40.9, 46.5, 59.3, 79.9, 118.8, 123.3, 123.8, 127.3, 129.2, 140.91, 153.20, 164.88, 173.12. MS (ESI): m/z (%): 375.24 (100) [$M+H^+$].

4.1.3 Generic synthesis of compounds 21-39

The appropriate compound 2-19 (0.2 mmol) was dissolved in a mixture of dioxane (15 mL) and HCl 4N (2 mL) and stirred for 24h at room temperature. Then the solvent was evaporated under vacuum and the solid residue was dissolved in H_2O and washed with ethyl acetate (3 x 10 mL). The aqueous layer was freeze-dried obtaining the desired compounds 21-39.

{1-[(3-{[(2-ammoniopropanoyl)amino]methyl}benzyl)amino]ethylidene}ammonium dichloride (1400W-Ala conjugate, **21**)

Yellow sticky solid, 85% yield. IR (KBr): 3424; 3178, 2980, 1683; ^{1}HNMR (300 MHz, CD_3OD) δ: 1.52 (d, J=7.2 Hz, 3H, CH_3), 2.27 (s, 3H, CH_3), 3.99 (q, J=6.6 Hz, H, CH), 4.44 (d, J=6.0, 4H, CH_2), 7.26-7.41 (m, 4H, CHAr, 8.58 (bs, 1H, NH); ^{13}CNMR (75 MHz, CD_3OD) δ: 16.5, 17.7, 42.7, 45.9, 49.1, 126.8, 127.1, 127.2, 129.1, 134.9, 139.3, 165.0, 169.8. Anal. calcd. for $C_{13}H_{22}Cl_2N_4O$: C 48.60, H 6.90, N 17.44; found C 48.57, H 6.88, N 17.39.

{1-[(3-{[(2-ammonio-3-methylpentanoyl)amino]methyl}benzyl)amino]ethylidene}ammonium dichloride (1400W-Ile conjugate, **22**)

Hygroscopic white solid, 80% yield. IR (KBr): 3442; 3098, 2918, 1680; ^{1}HNMR (300 MHz, CD_3OD) δ: 0.92-1.01 (m, 6H, CH_3), 1.2 (septet, J=7.2 Hz, 1H, HC*H*), 1.52-1.59 (m, 1H, *H*CH), 1.88-1.98 (m, 1H, CH), 2.27 (s, 3H, CH_3), 3.79 (d, J=5.4 Hz,1H, CH), 4.44 (t, J=6.6 Hz, 4H, CH_2), 7.27-7.41 (m, 4H, CHAr); 8.62 (s, 1H, NH), 9.15 (s, 1H, NH), 9.68 (s, 1H, NH); ^{13}CNMR (75 MHz, CD_3OD) δ: 10.5, 14.0, 17.8, 24.3, 36.9, 42.8, 45.9, 57.8, 126.9, 127.4, 127.6, 129.1, 134.9, 139,1, 139.2, 165.0, 168.3. Anal. calcd. for $C_{16}H_{28}Cl_2N_4O$:C 52.89, H 7.77, N 15.42; found C 52.84, H 7.72, N 15.39.

{1-[(3-{[(2-ammonio-4-methylpentanoyl)amino]methyl}benzyl)amino]ethylidene}ammonium dichloride (1400W-Leu conjugate, **23**)

Hygroscopic white solid, 87% yield. IR (KBr): 3425; 3154, 2974, 1678;^{1}HNMR (300 MHz, CD_3OD) δ: 0.99 (t, J=4.5 Hz, 6H, CH_3), 1.71 (d, J=5.7 Hz, 3H, CH and CH_2), 2.28 (s, 3H, CH_3), 3.95 (t, J=6.6 Hz, 1H, CH), 4.44-4.48 (m, 4H, CH_2), 7.27-7.41 (m, 4H, CHAr) 8.61 (bs, 1H, NH), 9.15 (bs, 1H, NH), 9.68 (bs, 1H, NH). ^{13}CNMR (75 MHz, CD_3OD) δ: 17.8, 21.8, 24.3, 40.5, 42.8, 45.9, 51.9, 126.8, 127.4, 127.5, 129.1, 134.9, 139.2, 164.9, 169.5. . Anal. calcd. for $C_{16}H_{28}Cl_2N_4O$: C 52.89, H 7.77, N 15.42; found C 52.91, H 7.76, N 15.40.

{1-[(3-{[(2-ammonio-3-methylbutanoyl)amino]methyl}benzyl)amino]ethylidene}ammonium dichloride (1400W-Val conjugate, **24**)

Hygroscopic white solid, 81% yield. IR (KBr): 3407; 3152, 2980, 1678; ^{1}HNMR (300 MHz, CD_3OD) δ: 1.02 (dd, J=6.9 Hz, 2.7 Hz, 6H, CH_3), 2.19 (sextet, J=6.9 Hz, 1H, CH), 2.28 (s, 3H, CH_3), 3.73 (d, J=6.6 Hz, 1H, CH), 4.43-4.47 (m, 4H, CH_2), 7.24-7.41 (m, 4H, CHAr), 8.61(bs, 1H, NH), 9.15 (bs, 1H, NH), 9.66 (bs, 1H, NH); ^{13}CNMR (75 MHz, CD_3OD) δ: 16.8, 17.7, 17.8, 30.4, 42.8, 45.8, 58.6, 126.9, 127.4, 127.6, 129.1, 135.0, 139.2, 165.0, 168.3. Anal. calcd. for $C_{15}H_{26}Cl_2N_4O$: C 64.71, H 9.41, N 20.13; found C 64.73, H 9.69, N 20.12.

(1-{[3-({[2-ammonio-4-(methylthio)butanoyl]amino}methyl)benzyl]amino}ethylidene)ammonium dichloride (1400W-Met conjugate, **25**)

Yellow sticky solid, 97% yield; IR (KBr): 3421; 3198, 2910, 1675; ^{1}HNMR (300 MHz, DMSO): δ 2.09 (s, 5H, CH_3SCH_2), 2.26 (s, 3H, CH_3), 2.51 (s, 2H, CH_2), 3.91 (bs, 1H, CH), 4.34 (dd, J=12.3 Hz, 4.8 Hz, 2H, CH_2), 4.46 (d, J=5.5 Hz, 2H, CH_2), 7.18- 7.37 (m, 4H, CHAr), 8.39 (bs, 3H, NH), 8.86 (s, 1H, NH), 9.19 (bs, 1H, NH), 9.29 (bs, 1H, NH), 10.0 (bs, 1H, NH); ^{13}CNMR (75 MHz, DMSO): δ 15.1, 19.3, 28.9, 31.5, 42.7, 45.6, 52.2, 127.18, 127.38, 127.5, 129.3, 136.2, 139.8, 164.7, 168.8. Anal. calcd. for $C_{15}H_{26}Cl_2N_4OS$: C 58.03, H 8.44, N 18.05; found C 58.00, H 8.47, N 18.08.

{1-[(3-{[(2-ammonio-3-mercaptopropanoyl)amino]methyl}benzyl)amino]ethylidene}ammonium dichloride (1400W-Cys conjugate, **26**)

Yellow sticky solid, 85% yield. IR (KBr): 3432; 3171, 2892, 1680;^{1}HNMR (300 MHz, CD_3OD) δ: 1.74 (t, J=4.5 Hz, 1H, SH), 2.27 (s, 3H, CH_3), 2.68-2.87 (m, 2H, CH_2), 3.76 (t, J= 5.5 Hz, 1H, CH), 4.47 (s, 4H, CH_2), 7.26-7.41 (m, 4H, CHAr), 8.61(bs, 1H, NH), 9.25 (bs, 1H, NH), 9.63 (bs, 1H, NH); ^{13}CNMR (75 MHz, CD_3OD) δ: 17.8, 40.4, 42.7, 45.9, 52.2, 126.8, 127.2, 127.3, 129.1, 134.9, 139.2, 165.0, 166.0. Anal. calcd. for $C_{13}H_{22}Cl_2N_4OS$: C 52.29, H 7.85, N 19.84; found C 52.31, H 7.82, N 19.83.

{1-[(3-{[(2-ammonio-3-hydroxypropanoyl)amino]methyl}benzyl)amino]ethylidene}ammonium dichloride (1400W-Ser conjugate, **27**)

Yellow sticky solid, 90% yield. IR (KBr): 3435, 3407, 2918, 1680;^{1}HNMR (300 MHz, DMSO) δ 2.26 (s, 3H, CH_3), 3.84 (q, J=6.3 Hz, 1H, CH), 3.93-4.02 (m, 2H, CH_2), 4.45 (d, J=2.7 Hz, 4H, CH_2), 7.25–7.41 (m, 4H, CHAr).^{13}CNMR (75 MHz, DMSO) δ 17.7, 42.8, 45.1, 55.1, 60.5, 126.8, 127.0, 127.2, 129.1, 134.9, 139.2, 165.0, 167.1 Anal. calcd. for $C_{13}H_{22}Cl_2N_4O_2$ C 58.62, H 8.33, N 21.04; found C 58.59, H 8.30, N 21.10.

{1-[(3-{[(2-ammonio-3-hydroxybutanoyl)amino]methyl}benzyl)amino]ethylidene}ammonium dichloride (1400W-Thr conjugate, **28**)

Yellow oil, 95% yield. IR (KBr): 3365, 3241, 3086, 1678; ^{1}HNMR (300 MHz, DMSO) δ 1.10 (d, J=6.3 Hz, 3H, CH_3), 1.21 (d, J=6.6 Hz, 1H, CH), 2.18 (s, 3H, CH_3), 3.91 (q, J=6.3 Hz, 1H, CH), 4.34 (d, J=6.0 Hz, 2H, CH_2), 4.46 (d, J=6.0, Hz, 2H, CH) 7.22-7.36 (m, 4H, CHAr), 8.23 (s, 3H, NH), 8.87 (s, 1H, NH) 9.18 (t, J=6.0 Hz, 1H, NH), 9.27 (s, 1H, NH), 10.02 (s, 1H, NH); ^{13}CNMR (75 MHz, DMSO): δ 19.3, 20.6, 42.7, 45.6, 59.0, 66.4, 127.1,127.4, 129.3, 136.1, 139.7, 164.7, 167.6. Anal. calcd. for $C_{14}H_{24}Cl_2N_4O_2$: C 47.87, H 6.89, N 15.95; found C 47.85, H 6.85, N 15.99.

{1-[(3-{[(4-amino-2-ammonio-4-oxobutanoyl)amino]methyl}benzyl)amino]ethylidene}ammonium dichloride (1400W-Asn conjugate, **29**)

Hygroscopic white solid, 76% yield. IR (KBr): 3394; 3171, 2979, 1683, 1674; ^{1}HNMR (300 MHz, DMSO) δ: 2.02 (s, 3H, CH_3), 2.67-3.03 (m, 2H, CH_2), 4.10 (bs, 1H, CH), 4.30 (d, J=5.4 Hz, 2H, CH_2), 4.47 (s, 2H, CH_2), 7.18-7.34 (m, 4H, CHAr); 8.30 (bs, 3H, NH), 8.95 (d, J=4.5 Hz, NH), 9.39 (s, 1H, NH), 10.11-10.16 (m, 1H, NH); ^{13}CNMR (75 MHz, DMSO) δ: 19.2, 36.1, 42.8, 45.5, 50.1, 127.0, 127.3, 129.3, 136.2, 136.3, 139.7, 164.7, 168.7, 171.4. Anal. calcd. for $C_{14}H_{23}Cl_2N_5O_2$: C 46.16, H 6.36, N 19.23; found C 46.21, H 6.41, N 19.20.

{1-[(3-{[(5-amino-2-ammonio-5-oxopentanoyl)amino]methyl}benzyl)amino]ethylidene}ammonium dichloride (1400W-Gln conjugate, **30**)

Hygroscopic white solid, 75% yield. IR (KBr): 3387; 3162, 2980, 1685; 1677; ^{1}HNMR (300 MHz, DMSO) δ: 1.84- 2.15 (m, 4H, CH_2), 2.18 (s, 3H, CH_3), 4.05 (q, J=3.9 Hz, 1H, CH), 4.27 (d, J=5.8, 2H, CH_2), 4.46 (d, J= 6.0, 2H, CH_2), 7.16-7.33 (m, 4H, CHAr), 8.67 (t, J=6.0 Hz, 1H, NH), 8.91 (d, J=6, 1H, NH), 9.37 (s, 1 H, NH), 10.05-10.18 (m, 1H, NH) ; ^{13}CNMR (75 MHz, DMSO) δ: 19.2, 25.9, 29.9, 42.6, 45.6, 56.4, 126.9, 127.1, 127.2, 129.2, 136.1, 140.4, 164.7, 173.1, 178.0. Anal. calcd. for $C_{15}H_{25}Cl_2N_5O_2$: C 47.62, H 6.66, N 18.51; found C 47.57, H 6.80, N 18.68.

[amino({4-ammonio-5-[(3-{[(1-iminioethyl)amino]methyl}benzyl)amino]-5-oxopentyl}amino)methylene]ammonium trichloride (1400W-Arg conjugate, **31**)

Hygroscopic white solid, 90% yield. IR (KBr) 3435, 3407, 2918, 1680; ^{1}HNMR (300 MHz, CD_3OD): δ 1.66-1.73 (m, 2H, CH_2), 1.86-2.02 (m, 2H, CH_2), 2.28 (s, 3H, CH_3), 3.27 (t, J=6.6 Hz, 2H, CH_2), 4.02 (t, J=6.6 Hz, 1H, CH), 4.38-4.53 (m, 4H, CH_2), 7.27- 7.42 (m, 4H, CHAr), 8.62 (bs, 1H, NH), 8.98 (bs, 1H, NH), 9.15 (bs, 1H, NH), 9.65 (bs, 1H, NH); ^{13}CNMR (75 MHz, CD_3OD): δ 17.8, 24.4, 28.6, 40.5, 42.8, 45.9, 52.9, 126.9, 127.5, 129.2, 134.9, 139.0, 157.4, 165.0, 168.6. Anal. calcd. for $C_{16}H_{30}Cl_3N_7O$ C 43.40, H 6.83, N 22.14; found C 43.52, H 6.78, N 22.20.

5-{2-ammonio-3-[(3-{[(1-iminioethyl)amino]methyl}benzyl)amino]-3-oxopropyl}-1H-imidazol-1-ium trichloride (1400W-His conjugate, **32**)

Hygroscopic white solid, 72% yield. 3385, 3107, 2918, 1675 ^{1}HNMR (300 MHz, CD_3OD): δ 2.27 (s, 3H, CH_3), 3.34-3.49 (m, 2H, CH_2), 4.31-4.38 (q, J=6.9 Hz, 1H, CH), 4.42-4.48 (m, 4H, CH_2), 7.24-7.40 (m, 4H, CHAr), 7.45 (s, 1H, CHAr), 7.53 (s, 1H, CHAr), 8.89 (s, 1H, NH), 8.93 (s, 1H, NH) . ^{13}CNMR (75 MHz, CD_3OD): δ 19.2, 26.0, 42.7, 45.5, 51.8, 118.2, 127.1,127.2, 127.8, 127.9, 128.4, 129.2, 134.7, 136.3, 139.4, 164.7, 170.3 Anal. calcd. for $C_{16}H_{25}Cl_3N_6O$: C 45.35, H 5.95, N 19.83; found C 45.48, H 6.07, N 19.95.

{1-[(3-{[(2-ammonio-3-phenylpropanoyl)amino]methyl}benzyl)amino]ethylidene}ammonium dichloride (1400W-Phe conjugate, **33**)

Yellow sticky solid, 90% yield. IR (KBr) 3353, 3093, 2932, 1678; ^{1}HNMR (300 MHz, DMSO): δ 2.18 (s, 3H, CH_3), 3.04 (t, J=6.6 Hz, 2H, CH_2), 4.06 (d, J=6.6 Hz 1H, CH), 4.26 (q, J= 2.4 Hz, 2H, CH_2), 4.42 (d, J=5.7 Hz, 2H, CH_2), 6.98 (d, J=7.5 Hz, 1H, CHAr), 7.20-7.32 (m, 8H, CHAr), 8.35 (s, 3H, NH), 8.83 (s, 1H, NH), 9.05 (t, J= 5.7 Hz, 1H, NH), 9.26 (s, 1H, NH), 9.93 (s, 1H, NH); ^{13}CNMR (75 MHz, DMSO): δ 19.3, 37.6, 42.6, 45.7, 54.2, 127.1, 127.3, 127.4, 127.8, 129.2, 129.3, 130.1, 135.6, 136.1, 139.4, 164.8, 168.6. Anal. calcd. for $C_{19}H_{26}Cl_2N_4O$: C 57.43, H 6.60, N 14.10; found C 57.48, H 6.68, N 14.07.

{1-[(3-{[(2,6-diammoniohexanoyl)amino]methyl}benzyl)amino]ethylidene}ammonium trichloride (1400W-Lys conjugate, **34**)

Hygroscopic white solid, 95% yield. IR (KBr): 3405, 3117, 2858, 1684; ^{1}HNMR (300 MHz, CD_3OD): δ 1.43-1.53 (m, 2H, CH_2), 1.66-1.76 (m, 2H, CH_2), 1.83-1.99 (m, 2H, CH_2), 2.28 (s, 3H, CH_3), 2.95 (t, J=7.2, 2H, CH_2), 4.00 (t, J= 6.6 Hz, 1H, CH), 4.37-4.54 (m, 4H, CH_2), 7.27-7.42 (m, 4H, CHAr), 8.62 (bs, 1H, NH), 9.17 (bs, 1H, NH), 9.67 (bs, 1H, NH); ^{13}CNMR (75 MHz, CD_3OD): δ 17.9, 21.8, 26.8, 30.9, 39.1, 42.8, 45.9, 53.0, 126.9, 127.4, 127.5, 129.1, 135.0, 139.1, 165.1, 168.8. Anal. calcd. for $C_{16}H_{30}Cl_3N_5O$: C 46.33, H 7.29, N 16.88; found C 46.39, H 7.25 N 16.91.

{1-[(3-{[(2-ammonio-3-carboxypropanoyl)amino]methyl}benzyl)amino]ethylidene}ammonium dichloride (1400W-Asp conjugate, **35**)

White solid, 90% yield, mp 123-125° C. IR (KBr): 3389, 3058, 2905, 1675; ^{1}HNMR (300 MHz, DMSO) δ 2.18 (s, 3H, CH_3), 2.81 (t, J=2.1 Hz, 2H, CH_2), 3.81 (q, J=5.5 Hz, 1H, CH), 4.31 (q, J=5.7 Hz, 2H, CH_2), 4.44 (d, J=5.7 Hz, 2H, CH_2), 7.21-7.35 (m, 4H, CHAr), 8.25 (s, 1H, NH), 9.05 (t, J=6.3 Hz, 1H, NH), 9.24 (s, 1H, NH), 9.96 (s, 1H, NH). ^{13}CNMR (75 MHz, DMSO) δ 19.3, 36.1, 42.8, 45.7, 52.6, 127.0, 127.2, 129.3, 136.1, 139.7, 164.8, 168.4, 171.7. Anal. calcd. for $C_{14}H_{22}Cl_2N_4O_3$: C 46.03, H 6.07, N 14.10; found C 46.07, H 6.11, N 14.07.

{1-[(3-{[(2-ammonio-4-carboxybutanoyl)amino]methyl}benzyl)amino]ethylidene}ammonium dichloride (1400W-Glu conjugate, **36**)

Yellow sticky solid, 95% yield. IR (KBr): 3396, 3089, 2915, 1681; ^{1}HNMR (300 MHz, DMSO) δ 1.90 (m, 2H, CH_2), 2.12 (s, 3H, CH_3), 2.24 (t, J=6.9 Hz, 2H, CH_2), 3.77-3.82 (m, 1H, CH), 4.14-4.39 (m, 4H, CH_2), 7.10-7.28 (m, 4H, CHAr), 8.35 (s, 3H, NH), 8.82 (s, 1H, NH), 9.17 (t, J= 5.7, 1H, NH), 9.26 (bs, 1H, NH), 9.99 (bs, 1H,

NH). ^{13}CNMR (75 MHz, DMSO) δ 19.2, 26.9, 29.8, 42.6, 45.5, 52.2, 127.1, 127.2, 127.4, 129.2, 136.2, 139.6, 164.6, 168.8, 173.8. Anal. calcd. for $C_{15}H_{24}Cl_2N_4O_3$: C 47.50, H 6.38, N 14.77; found C 47.59, H 6.36 N 14.62.

(1-{[3-({[2-ammonio-3-(4-hydroxyphenyl)propanoyl]amino}methyl)benzyl]amino}ethylidene)ammonium dichloride (1400W-Tyr conjugate, **37**)

Yellow sticky solid, 95% yield. IR (KBr): 3425, 3389; 3022, 2896, 1679. ^{1}HNMR (300 MHz, DMSO) δ 2.18 (s, 3H, CH_3), 2.91 (t, J=6.0 Hz, 2H, CH_2), 3.95 (m, 1H, CH), 4.26 (t, J= 5.1 Hz, 2H, CH_2), 4.43 (d, J=6.3 Hz, 2H, CH_2), 6.66 (d, J=8.1 Hz, 2H, CHAr), 7.01(d, J=8.4 Hz, 2H, CHAr), 7.22-7.31 (m, 4H, CHAr), 8.86 (s, 1H, NH), 9.14 (bs, 1H, NH), 9.26 (s, 1H, NH), 9.99 (bs, 1H, NH). ^{13}CNMR : (75 MHz, DMSO) δ 19.3, 34.8, 45.6, 46.8, 54.5, 125.5, 127.0, 127.3, 127.4, 129.2, 131.1, 136.0, 139.4, 157.2, 164.8, 168.7. Anal. calcd. for $C_{19}H_{26}Cl_2N_4O_2$ C 55.21, H 6.34, N 13.55; found C 55.27, H 6.42, N 13.63.

(1-{[3-({[2-ammonio-3-(1H-indol-3-yl)propanoyl]amino}methyl)benzyl]amino}ethylidene)ammonium dichloride (1400W-Trp conjugate, **38**)

Hygroscopic white solid, 75% yield; IR (KBr): 3399, 3088, 2912, 1685; ^{1}HNMR (300 MHz, CD_3OD) δ: 2.25 (s, 3H, CH_3), 3.35-3.48 (m, 2H, CH_2), 4.18 (t, J= 6.6 Hz, 1H, CH), 4.36 (s, 2H, CH_2), 4.42 (d, J= 5.1 Hz, 2H, CH_2), 7.02-7.67 (m, 9H, CHAr), 8.58 (bs, 1H, NH), 9.13 (bs, 1H, NH), 9.61 (bs, 1H, NH); ^{13}CNMR (75 MHz, CD_3OD) δ: 17.9, 27.7, 42.9, 46.0, 54.0, 106.8, 111.4, 118.1, 119.0, 121.7, 124.6, 126.8, 127.2, 127.4, 129.0, 134.8, 137.0, 138.8, 168.9, 170.4. Anal. calcd. for $C_{21}H_{27}Cl_2N_5O$: C 57.80, H 6.24, N 16.05; found C 57.87, H 6.29 N 15.95.

2-{[(3-{[(1-iminioethyl)amino]methyl}benzyl)amino]carbonyl}pyrrolidinium dichloride (1400W-Pro conjugate, **39**).

Pale yellow sticky solid. Yield 70%. IR (KBr):3379, 3108, 2914, 1681 cm^{-1}. ^{1}HNMR (300 MHz, DMSO) δ: 1.84 (m, 2H, CH_2), 2.20 (s, 3H, CH_3), 3.19 (q, J= 5.1 Hz, 1H, CH), 3.24 (pentet, J= 6.3 Hz, 4H, CH_2), 4.33 (d, J= 5.7 Hz, 2H, CH_2), 4.48 (d, J= 6.0 Hz, 2H, CH_2), 7.20-7.36 (m, 4H, CHAr), 8.81 (bs, 3H, NH), 8.93 (s, 1H, NH), 9.31 (t, J=6.3 Hz, 2H, NH), 10.09 (bs, 1H, NH); ^{13}CNMR (75 MHz, DMSO) δ: 19.2, 24.3, 30.2, 42.8, 46.6, 59.5, 63.4, 127.1, 127.2, 129.9, 136.3, 139.7,164.8, 168.7 Anal. calcd. for $C_{15}H_{24}Cl_2N_4O$: C 57.78, H 7.76, N 17.97; found: C 57.82, H 7.71, N 17.90.

4.2 Biological Sudies

4.2.1 Radiometric assay procedure

Recombinat murine iNOS and recombinant bovine eNOS were purchased from Bertin Pharma (Montigny-le-Bretonneux, France). Recombinat rat nNOS was purchased from Axxora Inc.(San Diego, CA). Enzymes were diluted in HEPES buffer (pH =7.4) to obtain a iNOS 100 μg/mL stock solution, and eNOS and nNOS 300 μg/mL stock solutions. Enzymatic assay was performed as previously described [24], with minor modifications. In

particular to perform iNOS enzymatic assay, 10 µL of enzyme stock solution were added to 80 µL of HEPES buffer pH = 7.4, containing 0.1 mM CaCl2, 1 mM DTT, 0.5 mg/mL BSA, 10 µM FMN; 10 µM FAD; 30 µM BH4, 10 µg/mL CaM and 10 µM L-Arginine. To measure constitutive NOSs, 25 µL of enzyme stock solution were added to 80 µL of HEPES buffer pH = 7.4, containing 2 mM CaCl2, 1 mM DTT, 0.5 mg/mL BSA, 10 µM FMN; 10 µM FAD; 30 µM BH4, 10 µg/mL CaM and 10 µM L-Arginine. For the citrulline radiometric detection, 2 µL of [H]^{3}L-arginine s.s. were added. To measure enzyme inhibition, a 10 µL solution of test compound (0.01 µM-10 µM) was added to the enzyme assay solution, followed by a pre-incubation time of 15 min at room temperature. The reaction was initiated by addition of 10 µL of NADPH 7.5 mM and was carried out at 37 °C for 20 min. Then it was stopped with 500 µL of ice-cold HEPES Na^+ pH=6 were added to the reaction, and [H]^{3}L- citrulline was separated by DOWEX, which was washed with 1,2 mL of water. 500 µL Aliquot of the eluate was added to 4 mL of scintillation fluid and the radioactivity was counted in a liquid scintillation counter. All assays were performed in triplicate.

4.2.2 Animal experiments

All experimental procedures involving animals were performed in accordance with Guidelines and Authorization for the Use of Laboratory Animals (Italian Government, Ministry of Health) and approved by the Committee on the Ethics of Animal Experiments of the University of Bari. Adult male Sprague-Dawley (SD) rats weighing 250- 300 g were obtained from Harlan Italy (Milan) and housed in a temperature-, humidity- and light-controlled room at the animal facility of our Department.

For experiments on LPS-treated animals, rats were injected i.p. with E. coli lipopolysaccharide (30 mg/kg diluted in 0.1 ml saline/100 g body weight). Four (4) hours later, rats were anesthetized with sodium pentobarbital (80 mg/kg body weight, i.p.), heparinized (400 UI/100g body weight, i.p.) and euthanized by cervical dislocation. All efforts were made to minimize animal suffering.

4.2.3 **Evaluation of Vascular Function *Ex Vivo***

Mesenteric vascular arteries (MVA) were isolated and removed as described [25]. Briefly, MVA mounted in a temperature-controlled moist chamber (type 834/1, Hugo Sachs Elektronik, March-Hungstetten, Germany) were perfused with modified Krebs-Henseleit solution continuously gassed with a mixture of 95% O_2 and 5% CO_2 (pH 7.4). A constant flow rate of 5 mL/min through the MVA was maintained using a peristaltic pump (ISM 833; Hugo Sachs Elektronik, March-Hungstetten, Germany). Drug solutions were infused into the perfusate proximal to the arterial cannula using another peristaltic pump. After an equilibration period (30 - 40 min), changes in perfusion pressure were measured with a Pressure Transducer System (SP 844 Capto, Horten, Norway) and recorded continuously using data acquisition and analysis equipment (PowerLab System, ADInstruments, Castle Hill, Australia).

4.2.4 Vasoconstrictor Responses in MVA

Dose-response curves measuring vasoconstriction (increase in PP) in response to NA were obtained by adding increasing concentrations of NA (10 nM - 10 µM /30 sec perfusion) to the perfusate. These experiments were also repeated after 30 min perfusion pre-treatment with compound 39 (0.06 µM), and subsequent treatment with L-NAME (100 µM). Relative changes in PP at steady-state reached with each dose of NA were measured and expressed in mmHg.

4.2.5 Statistical analysis

Results are expressed as mean ± SE of at least 4 independent experiments, repeated in duplicate, for each condition. All values were analyzed by a two-way repeated measures ANOVA. If the global tests showed major interactions, a one-factor ANOVA followed by Bonferroni correction analysis was performed between different treatments within the same time-point. Statistical differences were considered significant if P value was less than 0.05. All analysis were performed using Statistica Release 7 (Statsoft Institute Inc.)

4.3 Cells experiments

4.3.1 Cell culture

CTX/TNA2 rat astrocytes (ATCC® CRL-2006TM) and C6 rat glioma cell line (ECACC 92090409, Sigma Aldrich, Milan, Italy) were cultivated in DMEM High Glucose and Ham's F12 medium, respectively, supplemented with 10% fetal bovine serum, 1% penicillin/streptomycin and 1% L-glutamine (all purchased by EuroClone, Milan, Italy) at 37°C and 5% CO2.

4.3.2 MTT assay

Cell metabolic activity of CTX/TNA2 rat astrocytes and C6 rat glioma cells was assessed by MTT (3-(4,5-Dimethylthiazol-2-yl)-2,5-Diphenyltetrazolium Bromide) test (Sigma Aldrich, Milan, Italy). Cells were seeded (8x103/well) in a 96-well tissue culture-treated plate (Falcon®, Corning Incorporated, NY, USA) and let them adhere for 24 h. Next, medium was removed and the cell monolayer was incubated in the presence of loading concentrations of compound 39 (0-2 mM) for 24, 48 and 72 h, refreshing the medium every 24 h. After the exposure time, cells were incubated with 100 µl/well of MTT (1mg/ml) 1:10 with fresh growth medium for 4 h at 37 °C and 5% CO_2. Finally, the MTT solution was removed and replaced with 100 µl/well of DMSO. Cells were incubated for additional 20 minutes at 37 °C and 5% CO_2 and gently swirled for 10 minutes at room temperature. The optical density was measured at 540 nm by means of a spectrophotometer (Multiskan GO, Thermo Scientific, Monza, Italy). The results were expressed as the percentage of untreated cells (100%) and each experiment was performed three times in triplicate (n=9).

4.3.3 Lactate dehydrogenase (LDH) activity assay

C6 rat glioma cells were seeded and stimulated as previously described for the MTT test. After the exposure time, cell supernatants were collected, centrifugated at 450g for 4 minutes and stored on ice. In order to quantify the cytotoxicity of loading concentrations of compound 39 (0-2 mM), the CytoTox 96® Non-Radioactive

Cytotoxicity Assay (Promega Corporation, WI, USA) was performed. The CytoTox 96® Assay quantitatively measures lactate dehydrogenase (LDH), a stable cytosolic enzyme that is released upon cell lysis. Released LDH in culture supernatants is measured with a 30 minute coupled enzymatic assay, which results in the conversion of a tetrazolium salt (iodonitrotetrazolium violet; INT) into a red formazan product. The absorbance signal was measured at 490 nm with a spectrophotometer (Multiskan GO, Thermo Scientific, Monza, Italy). The results were expressed according to the formula: %LDH released=[(A–B)/(C–B)] ×100, with A=LDH activity of sample, B=LDH activity of growth medium (background) and C=LDH activity of the positive control (cell lysate).

4.3.4 Cell cycle analysis

Aiming to measure the proliferation rate of C6 rat glioma cells exposed to loading concentrations of compound 39, cell cycle progression was assessed by flow cytometry. Cells were seeded (2.4x105/well) in a 6-well tissue culture-treated plate (Falcon®, Corning Incorporated, NY, USA) and let them adhere for 24 h. Then growth medium was removed and replaced with fresh medium mixed with compound 39 (0-2 mM) every 24 h up to 72 h. After the exposure time, cells were washed twice with PBS without calcium and magnesium, harvested with Trypsin EDTA 1X (all purchased by EuroClone S.p.a., Milan, Italy) and counted by means of Trypan blue exclusion test (Sigma Aldrich, Milan, Italy). Approximately 5x105 cells/experimental condition were fixed with cold ethanol 70 % v/v and kept overnight at 4 °C. Cells were then resuspended in the staining solution made by PBS without calcium and magnesium, 1 mg/mL Propidium Iodide (final concentration 10 µg/mL) and 10 mg/mL RNAse (final concentration 100 µg/mL) and kept overnight at 4 °C. Cell cycle profiles (1x104 events/sample)were finally analyzed with a CytoFLEX Flow Cytometer (Beckman Coulter, FL, USA) and data were quantified using the FCS Express 5 Flow Cytometry Data Analysis (De Novo Software, CA, USA).

4.4 Docking Calculations

Docking calculations were performed using Glide v7.0 program [26-28]. The protein structures used in the docking studies were murine iNOS and taurine eNOS complexed with W1400 (pdb codes 1QW5 and 1F0I, respectively).

All crystal structures were prepared according to the protein preparation recommended procedure using Protein Preparation package [29, 30]. The ligands and solvent molecules were removed, but the cofactors, heme and tetrahydrobiopeterine (H_4B) for iNOS or glycerol (GOL) for eNOS were retained near the active site. Then, in the case of 1FOI, the GOL was replaced by coenzyme H_4B, after superimposition of the structure of 1FOI to 1QW5 (RMSD = 0.9811 Å).The resulting structure was optimized using the PR Conjugant Gradient (PRCG) method implemented in MacroModel [31]; extended cutoff distances were defined at 8 Å for van der Waals, 20 Å for electrostatics, and 4 Å for H-bonds. For each protein structure, polar hydrogen atoms were added, and atom charges were assigned based on OPLS-2005 force field. Hydrogens were also added to the heme and H4B. TheFe atom of heme was assigned a charge of +3. The protein structures were finally optimized using the same

parameters reported before. The ligand structures were prepared using LigPrep tool [32] in order to define the protonation state and atom charges (reference pH = 7.4 ± 0.5, OPLS-2005 force field). Docking was carried out in standard docking mode with the receptor after removal of the substrate. Potential steric clashes were alleviated via energy minimization with the OPLS-2005 force field.The binding region was defined by a 15 Å ×15 Å ×15 Å box centered on the mass center of the crystallographic ligand. Default input parameters were used in all computations (no scaling factor for the VdW radii of nonpolar protein atoms, 0.8 scaling factor for nonpolar ligand atoms).

All compounds were docked and scored using the Glide extra-precision (XP)12 mode and the best poses per ligand was chosen using the model energy score (Emodel) derived from a combination of the Glide Score (Gscore, a modified and extended version of the empirically based ChemScore function), Coulombic and the vander Waals energies, and the strain energy of the ligands. A conformational search of the ligand in the active siteof the protein was performed in order to gain the more stable ligand-protein poses. After the minimization of each structure, an extra-precision (XP) docking was carried out on the best pose.

Funding Sources

This study was supported by University "G. d'Annunzio" of Chieti local grants.

REFERENCES

[1] T.A. Heinrich, R.S. da Silva, K.M. Miranda, C.H. Switzer, A.D. Wink, J.M. Fukuto, Biological nitric oxide signaling: chemistry and terminology, Br. J. Pharmacol. 169 (2013) 1417-1429.

[2] U. Forstermann, W.C. Sessa, Nitric oxide synthases: regulation and function, Eur. Heart J. **33** (2012) 829–837.

[3] C. Maccallini, R. Amoroso, Targeting neuronal nitric oxide synthase as a valuable strategy for the therapy of neurological disorders, Neural Reg. Res. 11 (2016) 1731-1734.

[4] P. Barbanti, G. Egeo, C. Aurilia, L. Fofi, D. Della-Morte, Drugs targeting nitric oxide synthase for migraine treatment, Expert Opin. Investig. Drugs 23 (2014) 1141-1148.

[5] V.S. Ibba, A.M. Ghonim, K. Pyakurel, M.R. Lammi, A. Mishra, A.H. Boulares, Potential of inducible nitric oxide synthase as a therapeutic target for allergen-induced airway hyperresponsiveness: a critical connection to nitric oxide levels and PARP activity, Mediators of Inflamm. (2016) Article ID 1984703 http://dx.doi.org/10.1155/2016/1984703

[6] K.P. Pavlick, F.S. Laroux, J. Fuseler, R.E. Wolf, L. Gray, J. Hoffman, M.B. Grisham, Role of reactive metabolites of oxygen and nitrogen in inflammatory bowel disease, Free Radic. Biol. Med. 33 (2002) 311-322.

[7] A. Pandolfi, E.A. De Filippis, Chronic hyperglicemia and nitric oxide bioavailability play a pivotal role in pro-atherogenic vascular modifications, Genes Nutr. 2 (2007) 195-208.

[8] F. Ching, A.R. Diers, N. Hogg, Cancer cell metabolism and the modulating effects of nitric oxide, Free Radic. Biol. Med. 79 (2015) 324–336.

[9] F. Vannini, K. Kashfi, N. Nath, The dual role of iNOS in cancer, Redox Biol. 6 (2015) 334–343.

[10] A. Jahani-Asl, A. Bonni, iNOS: a potential therapeutic target for malignant glioma, Curr. Mol. Med. 13 (2013) 1241-1249.

[11] C. Maccallini, A. Patruno, A. Ammazzalorso, B. De Filippis, M. Fantacuzzi, S. Franceschelli, L. Giampietro, S. Masella, M.L. Tricca, R. Amoroso, Selective inhibition of inducible nitric oxide synthase by derivatives of acetamidine, Med. Chem. 8 (2012) 991-995.

[12] Y. Yang, T. Yu, Y. Lian, R. Ma, S. Yang, J.Y. Cho, Nitric oxide synthase inhibitors: A review of patents from 2011 to the present, Expert Opin. Ther. Pat. 25 (2015) 49-68.

[13] M.E. Camacho, M. Chayah, M.E. García, N. Fernández-Sáez, F. Arias, M.A. Gallo, M.D. Carrión, Quinazolinones, Quinazolinthiones, and Quinazolinimines as Nitric Oxide Synthase Inhibitors: Synthetic Study and Biological Evaluation, Arch. Pharm. 349 (2016) 638-650.

[14] N. Re, M. Fantacuzzi, C. Maccallini, R. Paciotti, R. Amoroso, Recent developments of amidine-like compounds as selective NOS inhibitors, Curr. Enzym. Inhib. 12 (2016), 30-39.

[15] R. Fedorov, E. Hartmann, D.K. Ghosh, I. Schlichting, Structural Basis for the Specificity of the Nitric-oxide Synthase Inhibitors W1400 and N^{ω}-Propyl-L-Arg for the Inducible and Neuronal Isoforms, J. Biol Chem. 278 (2003) 45818–45825.

[16] C. Maccallini, A. Patruno, N. Besker, J.I. Ali, A. Ammazzalorso, B. De Filippis, S. Franceschelli, L. Giampietro, M. Pesce, M. Reale, M.L. Tricca, N. Re, M. Felaco, R. Amoroso, Synthesis, biological evaluation, and docking studies of N-substituted acetamidines as selective inhibitors of inducible nitric oxide synthase, J.Med. Chem. 52 (2009), 1481−1485.

[17] C. Maccallini, A. Patruno, F. Lannutti, A. Ammazzalorso, B. De Filippis, M. Fantacuzzi, S. Franceschelli, L. Giampietro, S. Masella, M. Felaco, N. Re, R. Amoroso, N-Substituted acetamidines and 2-methylimidazole derivatives as selective inhibitors of neuronal nitric oxide synthase, Bioorg. Med. Chem. Lett. 20 (2010) 6495- 6499.

[18] M. Fantacuzzi, C. Maccallini, F. Lannutti, A. Patruno, S. Masella, M. Pesce, L. Speranza, A. Ammazzalorso, B. De Filippis, L. Giampietro, N. Re, R. Amoroso, Selective inhibition of iNOS by benzyl- and dibenzyl derivatives of N-(3-aminobenzyl)acetamidine, ChemMedChem 6 (2011) 1203−1206.

[19] C. Maccallini, M. Montagnani, R. Paciotti, A. Ammazzalorso, B. De Filippis, M. Di Matteo, S. Di Silvestre, M. Fantacuzzi, L. Giampietro, M.A. Potenza, N. Re, A. Pandolfi, R. Amoroso, Selective acetamidine-based nitric oxide synthase inhibitors: synthesis, docking, and biological studies, ACS Med. Chem. Lett. 6 (2015) 635−640.

[20] J. Haitao, L. Huiying, M. Flinspach, T.L. Poulos, R.B. Silverman, Computer modeling of selective regions in the active site of nitric oxide synthases: implication for the design of isoform-selective inhibitors, J. Med. Chem. 46 (2003) 5700−5711.

[21] Y. Zhu, D. Nikolic, R.B. Van Breemen, R.B. Silverman, Mechanism of inactivation of inducible nitric oxide synthase by amidines. Irreversible enzyme inactivation without inactivator modification, J. Am. Chem. Soc. 127, (2005) 858−868.

[22] D. Mitolo-Chieppa, M. Serio, M.A. Potenza, M. Montagnani, G. Mansi, S. Pece, E. Jirillo, J.C. Stoclet, Hyporeactivity of mesenteric vascular bed in endotoxin-treated rats. Eur. J. Pharmacol. 309 (1996) 175-182.

[23] J.N. Sarkaria, G.J. Kitange, C.D. James, R. Plummer, H. Calvert, M. Weller, W. Wick, Mechanisms of chemoresistance to alkylating agents in malignant glioma, Clin. Cancer. Res. 14 (2008) 2900-2908.

[24] C. Maccallini, M. Di Matteo, A. Ammazzalorso, A. D'Angelo, B. De Filippis, S. Di Silvestre, M. Fantacuzzi, L. Giampietro, A. Pandolfi, R. Amoroso, Reversed-phase high-performance liquid chromatography method with fluorescence detection to screen nitric oxide synthases inhibitors, J. Sep. Sci. 37 (2014) 1380-1385

[25] M.A Potenza, F.L. Marasciulo, D.M. Chieppa, G.S. Brigiani, G. Formoso, M.G. Quon, M. Montagnani, Insulin resistance in spontaneously hypertensive rats is associated with endothelial dysfunction characterized by imbalance between NO and ET-1 production. Am. J. Physiol. Heart Circ. Physiol. 289 (2005) 813-822.

[26] T.A. Halgren, R.B. Murphy, R.A. Friesner, H.S. Beard, L.L. Frye, W.T. Pollard, J.L. Banks, Glide: A New Approach for Rapid, Accurate Docking and Scoring. 2. Enrichment Factors in Database Screening, J. Med. Chem. 47 (2004) 1750–1759.

[27] R.A. Friesner, J.L. Banks, R.B. Murphy, T.A. Halgren, J.J. Klicic, D.T. Mainz, M.P. Repasky, E.H. Knoll, D.E. Shaw, M. Shelley, J.K. Perry, P. Francis, P.S. Shenkin, Glide: A New Approach for Rapid, Accurate Docking and Scoring. 1. Method and Assessment of Docking Accuracy. J. Med. Chem. 47 (2004) 1739–1749.

[28] Glide, version 7.0, Schrödinger, LLC, (2013) New York, NY.

[29] G.M. Sastry, M. Adzhigirey, T. Day, R. Annabhimoju, W. Sherman, Protein and ligand preparation: Parameters, protocols, and influence on virtual screening enrichments. J. Comput. Aid. Mol. Des. 27 (2013) 221- 234.

[30] Schrödinger Suite 2013 Protein Preparation Wizard; Epik version 2.4, Schrödinger, LLC, New York, NY, (2013) ; Impact version 5.9, Schrödinger, LLC, New York, NY, (2013); Prime version 3.2, Schrödinger, LLC,New York, NY, (2013).

[31] MacroModel, version 10.0, Schrödinger, LLC, New York, NY, (2013).

[32] LigPrep, version 2.6, Schrödinger, LLC, New York, NY, (2016).

LIST OF CAPTIONS

FIGURES

Fig. 1 Amidines inhibitors of iNOS

Fig.2 Acetamidines structurally related to 1400W

Fig.3. Chemical structures of target molecules

Fig.4. *Ex vivo* evaluation of 39 effects on NA-mediated vasoconstriction. Dose-response curves for NA- induced vasoconstriction (10 nM - 10 μM) were obtained in mesenteric vascular arteries (MVA) under basal conditions (CTRL), after pre-treatment with 39 and after subsequent treatment with L-NAME. Panel A. Maximal vasoconstriction to individual NA doses (peak ef-fect) was measured as perfusion pressure value and expressed in mmHg. Panel B. Duration of vasoconstriction obtained with individual NA doses (10 nM - 10 μM) was calculated as area under the curve (AUC) and expressed as perfusion pressure (mmHg) x time (sec). Results are mean ± SEM of duplicates from 4 experiments independently repeated.

Fig.5. Cell metabolic activity of CTX/TNA2 rat astrocytes and C6 rat glioma cells exposed to loading concentrations of 39. Metabolic activity of rat astrocytes (a) and C6 rat glioma cells (b) expressed as the ratio (%) of the untreated cells (0 mM compound **39** or 1400W) measured by the MTT test. Results represent the means ± SD (n=9). *p<0.05, **p<0.01, ***p<0.001 cells treated vs untreated cells.

Fig.6. Cytotoxicity and cell cycle progression of loading concentrations of 39 on C6 rat glioma cells. Left panel: cytotoxicity occurrence measured by the percentage of lactate dehydrogenase released from C6 rat glioma cells after 24-72 h of exposure to loading concentrations of **39**. Right panel: cell cycle progression of C6 rat glioma cells treated with increasing concentrations of compound **39** after 72h. Results represent the means ± SD (n=9). *$p<0.05$, **$p<0.01$ cells treated *vs* untreated cells.

Fig.7. Interactions responsible for the binding of **39** into the binding site of iNOS.

SCHEMES

Scheme 1. Synthesis of target molecules 21-39. Reagents and conditions. a:Boc-protected or Boc(OtBu)- protected amino acid, iBuOCOCl, NMM, DMF dry, N_2, -15 °C to r.t. , 18-24h; b: HCl 4N, 1,4 dioxane, r.t., 24 h.

TABLES

Table 1. Inhibition of iNOS and eNOS by 21-39: IC_{50} ad Selectivity

Table 2. Inhibition of nNOS by 39: IC50 and Selectivity